Lower mantle mineral associations in diamonds from São Luiz, Brazil

B. Harte,[1] J. W. Harris,[2] M. T. Hutchison,[1,3] G. R. Watt,[1,4] and M. C. Wilding[1,5]

[1]Department of Geology and Geophysics, University of Edinburgh, King's Buildings, Edinburgh EH9 3JW, UK
[2]Division of Earth Sciences, University of Glasgow, Lilybank Gardens, Glasgow G12 8QQ, UK
[3]Lunar and Planetary Laboratory, University of Arizona, Tucson, AZ 85721, USA
[4]School of Applied Geology, Curtin University of Technology, Perth 6845, W. Australia
[5]Thermochemistry Facility, University of California at Davis, Davis, CA 95616, USA

Abstract—A suite of diamonds from the São Luiz, alluvial deposit, Brazil, shows an unprecedented abundance of $(Mg,Fe)O$ (ferropericlase-magnesiowüstite - fPer) inclusions, which under normal circumstances are most likely to be derived from the lower mantle. Furthermore, occasional colourless inclusions in the same diamonds have compositions of $(Mg,Fe)SiO_3$ and $CaSiO_3$, corresponding to those of the phases MgSi-perovskite (MgSiPvk) and CaSi-perovskite (CaSiPvk), which are also expected to occur in the common peridotitic compositions of the lower mantle. Aluminous phases in the same suite of diamonds include: (1) a phase (TAPP) of garnet composition, $(Mg,Fe)Al_2Si_3O_{12}$ but with a distinct tetragonal crystal structure; (2) an Al-rich MgSiPvk; (3) an Al_2O_3 phase.

Unlike the occasional and always magnesian fPer inclusions reported in diamonds from other localities, the São Luiz fPer have an extremely wide range of composition, with $Fe^{2+}/(Fe^{2+} + Mg)$ ranging from 0.14 to 0.62. In some of these fPer inclusions very fine scale exsolution of a magnesioferrite spinel phase has been detected. The $CaSiO_3$ are exceptionally restricted in major-minor element compositions, and are close to pure $CaSiO_3$. MgSiPvk inclusions have Al_2O_3 ranging from 1.2 to 2.7 wt%, except in one case where it is 10.0%. The $Fe^{2+}/(Fe^{2+} + Mg)$ of MgSiPvk ranges from 0.02 to 0.05, so that Fe^{2+} is relatively distributed in favour of fPer as expected from experimental work. However, Mössbauer spectroscopic determinations show MgSiPvk and TAPP to have significantly higher proportions of Fe^{3+} than fPer, especially in the case of the high-Al MgSiPvk and TAPP. TAPP grains have $Fe^{2+}/(Fe^{2+} + Mg)$ of 0.03 to 0.06, with close to 3 Si cations in a 12 oxygen formula unit, and thus no sign of majoritic solid solution. Associations of fPer, MgSiPvk and SiO_2 in the same diamonds give phase relationships consistent with experimental data for lower mantle conditions. TAPP is unreported from experimental work.

Ion microprobe analysis of the inclusions for trace elements shows very low, generally less than chondritic, compositions for the fPer, MgSiPvk and TAPP. However, in CaSiPvk the REE contents are very high (ca. $200\times$ chondrite), in agreement with previous experimental work for lower mantle assemblages. A small positive Eu anomaly is seen in the CaSiPvk inclusions analysed. A calculated bulk pyrolite composition for the São Luiz assemblages gives trace element bulk compositions in between those of estimated primitive mantle and average OIB compositions. An ion microprobe oxygen isotope analysis on one CaSiPvk inclusion shows $\delta^{18}O$ of ca. 6 permil, consistent with expected mantle compositions. For the diamonds containing the inclusions, bulk $\delta^{13}C$ analyses yield typical mantle values.

Consideration of the inclusion associations found in the diamonds, in conjunction with ultra-high pressure experimental data, suggests that the natural mineral assemblages have come from a depth range of possibly less than 100km in the uppermost part of the lower mantle, with TAPP largely taking the place normally assigned to garnet (majoritic) in the upper part of this depth range. The possible stability range of TAPP is probably very restricted, being replaced with increasing depth by aluminous MgSiPvk in normal ultrabasic-basic compositions, on the basis of both the inclusion and experimental evidence. Thus within the uppermost lower mantle there is a shallower Al-poor MgSiPvk mineral facies, and a deeper Al-rich MgSiPvk mineral facies. The inclusions probably became encapsulated in diamond in this depth range.

The lower mantle São Luiz inclusion suite suggests that some material has formed from other sources (protoliths) besides expected lower mantle ultrabasic/pyrolite compositions. The Eu anomaly shown by the CaSiPvk inclusions may indicate an original crustal source. On the other hand, the very wide range in Fe/(Fe + Mg) of the fPer, and in particular the high Fe compositions may result from some derivation of material from the D″ layer at the mantle-core boundary. If these origins are correct, then the São Luiz data may suggest a mixing of some material of both crustal and D″ origins with pyrolitic mantle adjacent to lower/upper mantle boundary, which argues in favour of layered mantle convection.

INTRODUCTION

The Earth's lower mantle, at depths between approximately 660 and 2880 km, is the largest of the Earth's major subdivisions, and its chemical composition, mineralogy and rheology are of major importance in assessing its interplay with the upper mantle and core, and their effect on the state and history of the planet. Because of its inaccessibility, information on the constitution of the lower mantle is largely a matter of inference from geophysical, geochemical, crystal chemical and experimental data, and there is extensive evidence from these sources to suggest a lower mantle with a dominantly magnesian peridotite or pyrolite chemical

composition, which is mainly composed of the silicate $(Mg,Fe)SiO_3$ in the perovskite crystal structure (MgSi-perovskite or MgSiPvk) and the oxide $(Mg,Fe)O$ (e.g., RINGWOOD, 1982; RINGWOOD and IRIFUNE, 1988; POIRIER, 1992). In addition, a separate Ca-rich phase $(CaSiO_3$ in perovskite structure – CaSi-perovskite or CaSiPvk) is expected to occur, and in some circumstances a separate Al-rich phase.

In recent years a number of $(Mg,Fe)O$ mineral inclusions in diamonds have been reported which suggest the possibility of recovering and directly examining actual samples of lower mantle material. Attention on this possibility was focussed by SCOTT-SMITH et al. (1984), who presented data on two $(Mg,Fe)O$ inclusions in diamonds from Orroroo and suggested that an inclusion of $(Mg,Fe)SiO_3$ in the same diamond suite might represent a MgSi-perovskite which had co-existed with MgFe-oxide in the lower mantle. MOORE et al. (1986) reported six further inclusions of $(Mg,Fe)O$ composition from three localities (Koffiefontein, Monastery and Sloane), including one diamond from Koffiefontein which contained inclusions of $(Mg,Fe)O$ and (Mg,Fe)-SiO_3 in the same diamond though not in contact with one another. Most recently $(Mg,Fe)O$ inclusions have been reported from São Luiz (WILDING et al., 1991; HARTE and HARRIS, 1994; HARRIS et al., 1997), Letseng-La-Terai (MCDADE and HARRIS, in press), Mwadui (STACHEL et al., 1998) and Guinea (HUTCHISON, 1997).

Up to the present, the São Luiz diamonds are proving the most exceptional for the abundance and variety of $(Mg,Fe)O$ inclusions recovered and the occurrence of both $(Mg,Fe)O$ and silicate inclusions in the same diamond. The São Luiz diamonds have been recovered from alluvial deposits near Aripuena, Mato Grosso, Brazil, and are associated with river gravels on the São Luiz river, which drains into the Amazon via the Aripuena river. The diamonds are thought to have been derived from Cretaceous kimberlites, which intrude through Proterozoic crustal rocks belonging to the Aripuena province. In addition to the occurrence of lower mantle mineral associations, diamonds from the São Luiz deposit have proved remarkable in also showing large proportions of inclusions of garnet with variable solid solution of pyroxene ('majorite' substitution) and thus implying formation within the transition zone of the upper mantle (WILDING et al., 1991; HARTE, 1992).

This paper will concentrate on the São Luiz mineral associations suggesting a lower mantle origin. Although MgSiPvk is expected to be the most abundant lower mantle phase, we have focussed attention in these studies on diamonds containing $(Mg,Fe)O$ inclusions. This is because MgSiPvk has compositions, dominantly Mg-SiO_3 with $FeSiO_3$ in solid solution, overlapping those of orthopyroxene (enstatite-hypersthene solid solution)

which is an abundant phase in the upper part of the upper mantle and occurs in diamonds of upper mantle origin (e.g., MEYER, 1987). To distinguish MgSiPvk and orthopyroxene inclusions on the basis of chemistry without crystal structure is therefore not possible; nor would crystal structure data provide unequivocal evidence of origin, since inversion of MgSiPvk inclusions to pyroxene structure may be expected during their transport to the Earth's surface. On the other hand, although $(Mg,Fe)O$ oxides have a wide pressure-temperature stability field in Si-poor compositions, they are only expected to occur in normal mantle ultrabasic compositions in the lower mantle (e.g., RINGWOOD and IRIFUNE, 1988), and may therefore provide a surer guide to material of potential lower mantle origin than the occurrence of inclusions with $(Mg,Fe)SiO_3$ compositions. $(Mg,Fe)O$ inclusions also have the merit of commonly being semi-opaque and sometimes having irridescent blue colours, which makes them relatively easy to identify within the diamonds before breaking of the diamonds for extraction of inclusions.

The focus of the work presented here is upon mineral compositions and associations, with only a little work on crystallographic structure incorporated. Thus we circumstantially identify potential lower mantle originally perovskite-structured inclusions (MgSiPvk and Ca-SiPvk) on the basis of their chemical composition, coupled with their occurrence in diamonds also containing $(Mg,Fe)O$ inclusions. Present evidence from X-ray diffraction studies suggests that both MgSiPvk and Ca-SiPvk inclusions reported herein now have lower pressure pyroxene structures (R. ANGEL and N. ROSS, pers. comm., 1993; P. CONRAD and R. HEMLEY, pers. comm. 1997), and have therefore inverted from the perovskite structure upon transport from the lower mantle. Further studies on the crystallographic structure of lower mantle suite of São Luiz inclusions, using within-diamond and synchrotron X-ray techniques developed for small inclusions, are presently being undertaken.

METHODS

The inclusions were broken out of the diamonds in a custom built sealed stainless steel crusher, following standard techniques (HARRIS and GURNEY, 1979). After breakout individual inclusions were examined and described and then mounted in araldite within small brass cylinders ('pips') with an internal diameter of 2.6 mm and a length of 4.8 mm. The upper surfaces of the inclusions were then polished in preparation for electron and ion microprobe analysis, as well as for SEM and TEM examination in some cases.

Electron microprobe analyses were conducted at the Department of Geology and Geophysics, University of Edinburgh, using Cambridge Instruments Microscan V and Cameca Camebax instruments, at 30 nA and 20 nA respectively and 20 kV. Metal (Cr, Ni, Fe, Ti, Mn, Fe), oxide (MgO, Al_2O_3) and silicate $(CaSiO_3, NaAlSi_3O_8, KAlSi_3O_8)$

standards were used in electron microprobe analysis and ZAF and PAP correction procedures were followed.

Trace element and oxygen isotope analyses were made using SIMS techniques at the Edinburgh University/NERC Ion Microprobe Facility. For trace elements an O^- primary beam was used and high energy secondary ions collected following the techniques described by HARTE and KIRKLEY (1997), who also provide information on error ranges. Ion yields were calculated relative to Si for silicates and relative to Mg for (Mg,Fe) oxide. The oxygen isotope analysis of a $CaSiO_3$ (originally CaSiPvk) inclusion was made using a Cs primary beam and following the techniques described by VALLEY et al. (1998). A wollastonite ($CaSiO_3$), provided by JOHN VALLEY (University of Wisconsin-Madison), was used as a standard in the oxygen isotope analysis.

DIAMOND SAMPLES AND MINERAL ASSOCIATIONS IN DIAMONDS

The data reported for São Luiz herein come very largely from two sets of inclusions obtained from diamonds with specimen numbers BZ65 to BZ120, and BZ201 to BZ214, respectively broken out of diamonds by WILDING and HARRIS and WATT and HARRIS. Some data on an additional set of inclusions, more recently broken out of diamonds by HUTCHISON and HARRIS and published in HARRIS et al. (1997) and McCAMMON et al. (1997), will also be considered. Recently gathered data on associations involving unusual pyroxene-like compositions and possible associations transitional between the upper and lower mantle (HUTCHISON, 1997) will be presented elsewhere (HUTCHISON et al., in prep.).

The above diamond specimens were selected for detailed study because their inclusions were sufficiently large to be broken out of the diamonds and analysed, as well forming part of a suite with abundant (Mg,Fe)O inclusions. Colourless inclusions in the diamonds containing (Mg,Fe)O were found to have chemical compositions of $(Mg,Fe)SiO_3$, $CaSiO_3$, and SiO_2. In addition some inclusions of green colour occurring in the same diamond as (Mg,Fe)O were found to have the composition of a pyrope-almandine garnet and are referred to herein by the acronym TAPP (tetragonal almandine-pyrope phase, see below). In addition to inclusions confirmed as occurring with (Mg,Fe)O, the specimen series BZ65 to BZ214 yielded some other colourless inclusions: two inclusions of $(Mg,Fe)_2SiO_4$, four of Ca-rich pyroxene composition, and one with an unstable Ca-Al-rich composition. Since these phases were not confirmed as occurring in diamonds containing (Mg,Fe)O, there is no particular evidence to associate them with the lower mantle, and they are omitted from further discussion in this paper. WATT et al. (1994) also reported the occurrence of an inclusion with Al_2O_3 composition from a diamond that lacked a (Mg,Fe)O phase. Some further inclusions, which were too small for reliable break out from the above diamonds, are now being considered for investigation by synchrotron X-ray techniques.

The chemical compositions of all inclusions investigated are given in Table 1 (MgFe oxides) and Table 2 (silicate phases), together with notes on which inclusions came from the same diamond. Particular significance is attached to the association of mineral inclusions in one diamond, and the associations reported here have all been confirmed by electron microprobe analysis subsequent to break out from the diamond. Associated inclusions in diamonds from higher levels of the mantle have commonly been interpreted as having been in equilibrium with one another (e.g., MEYER, 1987; GURNEY, 1989) even though the different mineral inclusions are usually separated by diamond and not in contact with one another. However evidence

of exceptions to this interpretation do occur (e.g., STACHEL et al., 1998), and some exceptions occur in the present inclusion suite. In particular, one diamond (BZ205) contained two (Mg,Fe)O inclusions with different compositions, which clearly could not be in equilibrium. It must be noted that in the present suite of material associated inclusions were only in actual contact with one another on one occasion (specimen BZ207 with MgSiPvk and TAPP in contact). Further evidence regarding equilibrium between associated inclusions will be discussed below.

Table 3 gives a summary list of all the inclusions and identifies the mineral associations seen in single diamonds and their frequency of occurrence. The terminology used is appropriate for perovskite-bearing (MgSiPvk and CaSiPvk) mineral assemblages of the lower mantle even though the inclusions from diamonds now commonly appear to be in a low pressure structural state (see above). TAPP is for tetragonal almandine-pyrope phase (HARRIS et al., 1997). Note also that we refer to (Mg,Fe)O compositions as ferroperoclases (fper); this conforms to normal mineralogical practice since the oxides are typically MgO rich and close to periclase (MgO), but there has been a tendency in the literature to refer to similar lower mantle (Mg,Fe)O phases as magnesiowüstite (MW). The list of $Fe^{2+}/(Fe^{2+} + Mg)$ compositions of (Mg,Fe)O in mineral associations given in Table 3 discounts occasional situations where the inclusions inside one diamond do not appear to be in equilibrium.

MINERAL CHEMISTRY— MAJOR/MINOR ELEMENTS

Abbreviations

Fe^t	total Fe atoms.
FeO^t	total Fe calculated as ferrous oxide.
[6]	coordination number of atomic site (six in this case).
$D_{Fe2+}^{MgSiPvk/fPer}$	partition coefficient of Fe^{2+} for MgSiPvk/fPer calculated as cations $Fe^{2+}/(Fe^{2+} + Mg)$.
$D_{Fe2+*}^{MgSiPvk/fPer}$	partition coefficient for Fe^{2+} between MgSiPvk and fPer calculated on basis of cations Fe^{2+} per formula unit; $RSiO_3$ and RO being the standard formula units for MgSiPvk and fPer, where 'R' indicates cations.

For tabulation of partition coefficients for other cations and phases see Table 4.

(Mg,Fe)O minerals

Electron microprobe analyses. Table 1 gives the compositions of 24 fPer from São Luiz, and 12 fPer given in the literature from other localities: Koffiefontein, Monastery, and Letseng La Terai in southern Africa (MOORE et al., 1986; McDADE and HARRIS, in press); Mwadui, Tanzania (STACHEL et al., in press); Guinea, West Africa (HUTCHISON, 1997); Orroroo,

Table 1: Oxide (Ferropericlase-magnesiowustite) Compositions for Sao Luiz and other locations.

Locality	Sao Luiz	Sao Luiz	Sao Luiz	Sao Luiz	Sao Luiz	Sao Luiz	Sao Luiz	Sao Luiz	Sao Luiz	Sao Luiz	Sao Luiz	Sao Luiz	Sao Luiz
Sample (BZ prefix for Sao Luiz)	BZ65	BZ66	BZ67	BZ69	BZ70	BZ72	BZ73	BZ74	BZ76	BZ78	BZ80	BZ287	BZ88
Phase	fPer	fPer	fPer	fPer	fPer	fPer	fPer	fPer	fPer	fPer	fPer	fPer	fPer
Other inclusions													
Wt %													
SiO2	0.00	0.01	0.00	0.00	0.05	0.00	0.02	0.00	0.03	0.00	0.00	0.00	0.00
TiO2	0.03	0.01	0.01	0.02	0.00	0.02	0.02	0.00	0.01	0.02	0.02	0.01	0.02
Al2O3	0.00	0.13	0.06	0.00	0.13	0.00	0.04	0.05	0.08	0.00	0.00	0.00	0.10
Cr2O3	0.30	1.06	0.03	0.50	0.79	0.30	0.38	0.30	0.81	0.80	0.40	0.50	0.00
FeOt	45.36	73.56	59.80	23.33	41.51	43.26	43.35	50.04	32.08	31.22	35.73	25.20	44.98
MnO		0.80	0.28		0.21		0.10	0.22	0.34				
NiO	0.30	0.10	0.28	1.02	0.49	0.26	0.40	0.53	1.21	0.89	0.74		
MgO	54.81	23.13	39.75	76.19	57.33	54.74	56.37	50.00	65.25	66.85	62.41	75.08	54.43
CaO		0.01	0.00		0.00		0.00	0.02	0.00				
Na2O		1.05	0.11		0.07		0.06	0.06	0.82				
K2O													
Total	100.80	99.87	100.32	101.06	100.55	98.58	100.73	101.21	100.60	99.78	99.30	100.79	99.53
Cations													
Si	0.000	0.000	0.000	0.000	0.000	0.000	0.000	0.000	0.000	0.000	0.000	0.000	0.000
Ti	0.000	0.000	0.000	0.000	0.000	0.000	0.000	0.000	0.000	0.000	0.000	0.000	0.000
Al	0.000	0.002	0.001	0.000	0.001	0.000	0.000	0.001	0.001	0.000	0.000	0.000	0.001
Cr	0.002	0.008	0.000	0.003	0.005	0.002	0.002	0.002	0.005	0.005	0.003	0.003	0.000
Fet	0.316	0.616	0.455	0.145	0.285	0.306	0.299	0.356	0.210	0.205	0.241	0.158	0.316
Mn		0.007	0.002		0.001		0.001	0.002	0.002				
Ni	0.002	0.001	0.002	0.006	0.003	0.002	0.003	0.004	0.008	0.006	0.005		
Mg	0.680	0.345	0.538	0.846	0.702	0.690	0.693	0.635	0.762	0.784	0.751	0.839	0.682
Ca		0.000	0.000		0.000		0.000	0.000	0.000				
Na		0.020	0.002		0.001		0.001	0.001	0.012				
K													
Total	1.000	1.000	1.000	1.000	1.000	1.000	1.000	1.000	1.000	1.000	1.000	1.000	1.000
Ferric - Ferrous													
Fe3+/Fet	0.02	0.07	0.02	0.02	0.02	0.02	0.02	0.02	0.02	0.02	0.02	0.02	0.02
Fe3+	0.006	0.012	0.009	0.003	0.006	0.006	0.006	0.007	0.004	0.004	0.005	0.003	0.006
Fe2+	0.309	0.604	0.445	0.142	0.280	0.300	0.293	0.349	0.206	0.201	0.236	0.155	0.310
Wt% Fe2O3	1.01	5.72	1.33	0.52	0.92	0.96	0.96	1.11	0.71	0.69	0.79	0.56	1.00
Wt% FeO	44.45	68.41	58.61	22.86	40.67	42.39	42.49	49.04	31.43	30.60	35.02	24.70	44.08
Fe2+/(Fe2+ + Mg)	0.313	0.624	0.453	0.144	0.285	0.303	0.297	0.355	0.213	0.204	0.239	0.156	0.312

Other inclusions refer to inclusions in the same diamond.
Absence of a number means element not anlysed. Fet refers to total Fe.
Ferric-ferrous ratios are based on McCammon et al. (1997) with average Fe3+/Fet value taken as 0.02.

Table 1: Oxide (Ferropericlase-magnesiowustite) Compositions for Sao Luiz and other locations - contd.

Locality	Sao Luiz	Sao Luiz	Sao Luiz	Sao Luiz	Sao Luiz	Sao Luiz	Sao Luiz	Sao Luiz	Sao Luiz	Sao Luiz	Sao Luiz
Sample (BZ prefix for Sao Luiz)	BZ103A	BZ116A	BZ120A	BZ201A	BZ205B	BZ205C	BZ206A	BZ207B	BZ210A	BZ238B	BZ251A
Phase	fPer	fPer	fPer	fPer	fPer	fPer	fPer	fPer	fPer	fPer	fPer
Other inclusions	SiO2	CaSiPvk	MgSiPvk		fPer + TAPP	fPer + TAPP	TAPP	TAPP+ MgSiPvk	MgSiPvk	TAPP	MgSiPvk
Wt %											
SiO2	0.01	0.02	0.00	0.02	0.02	0.05	0.05	0.03	0.05	0.07	0.04
TiO2	0.01	0.00	0.00	0.03	0.01	0.02	0.02	0.02	0.01	0.04	0.01
Al2O3	0.03	0.03	0.04	0.04	0.07	0.23	0.14	0.11	0.13	0.12	0.04
Cr2O3	0.37	0.75	0.75	0.15	0.77	2.56	1.41	0.51	1.33	0.66	0.34
FeOt	43.47	28.77	42.81	49.95	27.72	49.26	27.34	43.14	27.20	26.37	23.52
MnO	0.10	0.18	0.41	0.16	0.35	0.30	0.35	0.43	0.29	0.36	0.22
NiO	0.36	1.33	0.77	0.34	1.25	0.70	1.23	0.90	1.27	1.40	1.25
MgO	55.38	67.94	55.25	48.91	69.14	46.84	69.01	54.84	69.22	71.31	74.77
CaO	0.01	0.00	0.00	0.01	0.02	0.00	0.00	0.01	0.01	0.00	0.02
Na2O	0.05	0.39	0.54	0.02	0.49	0.05	1.25	0.14	0.87	0.12	0.18
K2O				0.00	0.01	0.01	0.01	0.00	0.00	0.00	0.01
Total	99.79	99.42	100.55	99.63	99.86	100.02	100.80	100.13	100.38	100.45	100.40
Cations											
Si	0.000	0.000	0.000	0.000	0.000	0.000	0.000	0.000	0.000	0.001	0.000
Ti	0.000	0.000	0.000	0.000	0.000	0.000	0.000	0.000	0.000	0.000	0.000
Al	0.000	0.000	0.000	0.000	0.001	0.002	0.001	0.001	0.001	0.000	0.000
Cr	0.002	0.005	0.005	0.001	0.005	0.018	0.009	0.003	0.008	0.004	0.002
Fet	0.304	0.188	0.296	0.362	0.179	0.360	0.175	0.301	0.175	0.169	0.148
Mn	0.001	0.001	0.003	0.001	0.002	0.002	0.002	0.003	0.002	0.002	0.001
Ni	0.002	0.008	0.005	0.002	0.008	0.005	0.008	0.006	0.008	0.009	0.008
Mg	0.689	0.791	0.682	0.632	0.797	0.611	0.786	0.682	0.793	0.813	0.838
Ca	0.000	0.000	0.000	0.000	0.000	0.000	0.000	0.000	0.000	0.000	0.000
Na	0.001	0.006	0.009	0.000	0.007	0.001	0.019	0.002	0.013	0.002	0.003
K				0.000	0.000	0.000	0.000	0.000	0.000	0.000	0.000
Total	1.000	1.000	1.000	1.000	1.000	1.000	1.000	1.000	1.000	1.000	1.000
Ferric - Ferrous											
Fe3+/Fet	0.02	0.02	0.02	0.02	0.02	0.02	0.02	0.02	0.02	0.03	0
Fe3+	0.006	0.004	0.006	0.007	0.004	0.007	0.003	0.006	0.003	0.003	0.003
Fe2+	0.298	0.184	0.290	0.355	0.176	0.353	0.171	0.295	0.171	0.165	0.145
Wt% Fe2O3	0.97	0.64	0.95	1.11	0.62	1.09	0.61	0.96	0.60	0.88	0.00
Wt% FeO	42.60	28.20	41.95	48.95	27.16	48.27	26.80	42.28	26.65	25.58	23.52
Fe2+/(Fe2+ + Mg)	0.301	0.189	0.299	0.360	0.181	0.366	0.179	0.302	0.178	0.168	0.150

Other inclusions refer to inclusions in the same diamond.

Absence of a number means element not anlysed. Fet refers to total Fe.

Ferric-ferrous ratios are based on McCammon et al. (1997) with average Fe3+/Fet value taken as 0.02.

Table 1: Oxide (Ferropericlase-magnesiowustite) Compositions for Sao Luiz and other locations - contd.

Locality	Koffiefontein	Koffiefontein	Koffiefontein	Koffiefontein	Ororoo	Ororoo	Sloane	Monastery	Letseng	Mwadui	Guinea	Guinea
Sample	A262	K30	K33	K34	ORR6A	ORR4A	A100	AI-40	LLT32A	MW56-82	GU2A	GU4A1
Phase	fPer	fPer	fPer	fPer	fPer	fPer	fPer	fPer	fPer	fPer	fPer	fPer
Other inclusions	MgSiPvk											
Wt %												
SiO_2	0.00	0.08	0.09	0.13	0.00	0.00	0.00	0.00	0.20	0.01	0.01	0.01
TiO_2	0.00	0.00	0.00	0.00	0.00	0.00	0.00	0.17	0.01	0.01	0.00	
Al_2O_3	0.00	0.00	0.00	0.07	0.01	0.00	0.10	0.17	0.09	0.02	0.02	0.06
Cr_2O_3	0.57	0.49	0.52	0.67	0.16	0.23	0.84	0.00	0.43	0.16	0.38	0.75
$FeOt$	19.80	21.70	20.50	20.30	21.13	22.92	19.40	93.00	18.29	22.19	20.39	20.85
MnO	0.19	0.15	0.16	0.17	0.15	0.16	0.32	0.32	0.12	0.12	0.14	0.19
NiO	1.41				1.20	1.10				1.27	1.38	1.41
MgO	78.10	77.30	76.80	76.90	77.70	76.75	78.70	7.29	79.37	75.59	77.62	76.81
CaO	0.00	0.00	0.05	0.03	0.00	0.00	0.04	0.00	0.00	0.01	0.01	
Na_2O	0.30	0.29	0.25	0.20	0.00	0.00	0.07		0.36	0.07	0.21	
K_2O		0.00	0.06	0.00	0.00	0.00	0.00		0.00	0.01		
Total	100.37	100.01	98.43	98.47	100.35	101.16	99.47	100.95	100.36	99.46	100.16	100.08
Cations												
Si	0.000	0.001	0.001	0.001	0.000	0.000	0.000	0.000	0.001	0.000	0.000	0.000
Ti	0.000	0.000	0.000	0.000	0.000	0.000	0.000	0.001	0.000	0.000	0.000	
Al	0.000	0.000	0.000	0.001	0.001	0.000	0.001	0.002	0.001	0.001	0.000	0.001
Cr	0.003	0.003	0.003	0.004	0.001	0.001	0.005	0.000	0.002	0.001	0.002	0.004
Fet	0.122	0.135	0.129	0.128	0.131	0.142	0.120	0.872	0.112	0.140	0.127	0.130
Mn	0.001	0.001	0.001	0.001	0.001	0.001	0.002	0.003	0.001	0.001	0.001	0.001
Ni	0.008				0.007	0.007			0.009	0.008	0.008	0.008
Mg	0.860	0.856	0.862	0.862	0.860	0.849	0.870	0.122	0.868	0.849	0.859	0.855
Ca	0.000	0.000	0.000	0.000	0.000	0.000	0.000	0.000	0.000	0.000	0.000	
Na	0.004	0.004	0.004	0.003	0.000	0.000	0.001	0.000	0.005	0.001	0.003	
K	0.000	0.000	0.001	0.000	0.000	0.000	0.000		0.000	0.000		
Total	1.000	1.000	1.000	1.000	1.000	1.000	1.000	1.000	1.000	1.000	1.000	1.000
Ferric - Ferrous												
Fe^{3+}/Fet	0.02	0.02	0.02	0.02	0.02	0.02	0.02	0.02	0.02	0.02	0.02	0.02
Fe^{3+}	0.002	0.003	0.003	0.003	0.003	0.003	0.002	0.017	0.002	0.003	0.003	0.003
Fe^{2+}	0.120	0.132	0.126	0.125	0.129	0.139	0.118	0.854	0.110	0.137	0.124	0.128
Wt% Fe_2O_3	0.44	0.48	0.46	0.45	0.47	0.51	0.43	2.07	0.41	0.49	0.45	0.46
Wt% FeO	19.40	21.27	20.09	19.89	20.71	22.46	19.01	91.14	17.92	21.75	19.98	20.43
$Fe^{2+}/(Fe^{2+} + Mg)$	0.122	0.134	0.128	0.127	0.130	0.141	0.119	0.875	0.112	0.139	0.126	0.130

Other inclusions refer to inclusions in the same diamond.

Absence of a number means element not anlysed. Fet refers to total Fe.

Ferric-ferrous ratios are based on McCammon et al. (1997) with average Fe3+/Fet value taken as 0.02.
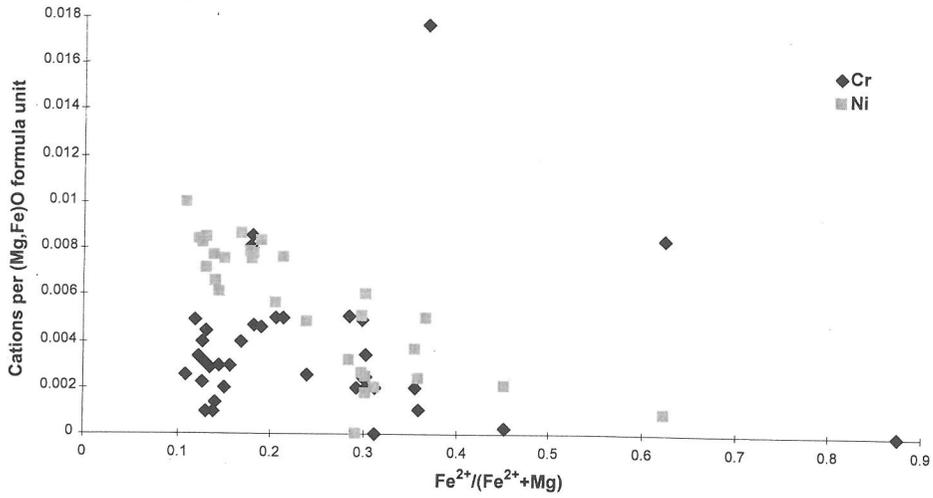
FIG. 1. Ni and Cr cations [for one (Mg,Fe)O formula unit], plotted against $Fe^{2+}/(Fe^{2+} + Mg)$ for fPer (all fPer data from Table 1).
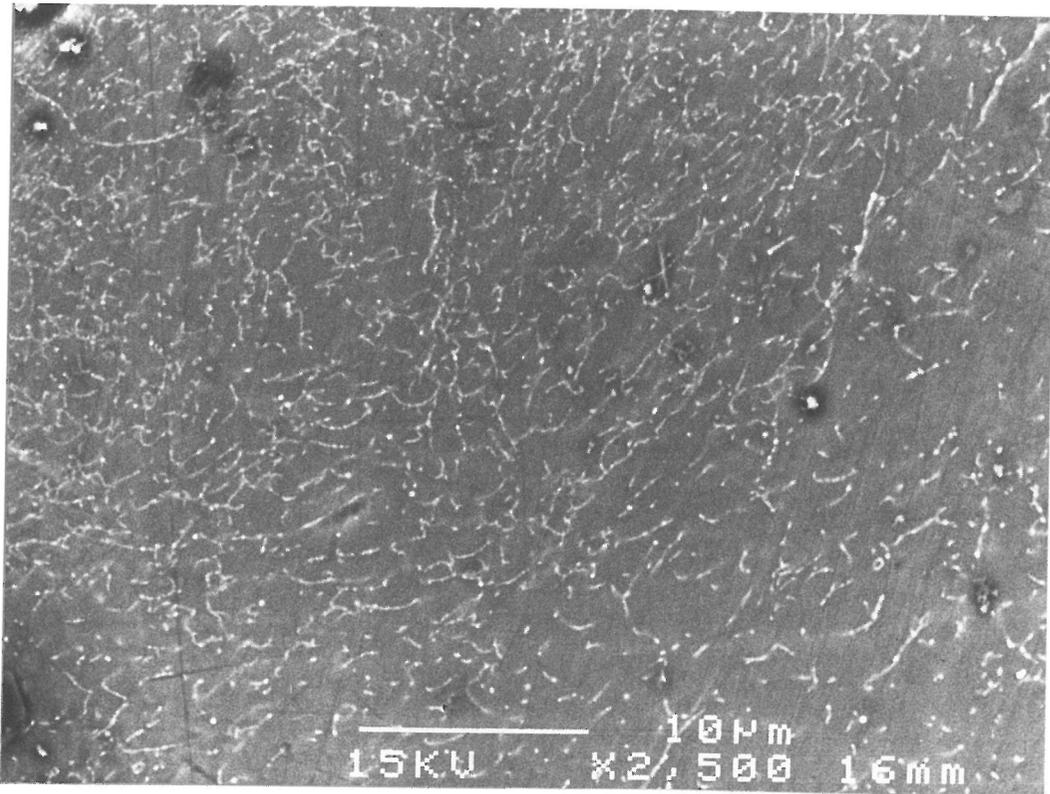
FIG. 2. Photograph of SEM backscatter image, showing small elongate bodies of magnesioferrite with high backscatter intensity in darker fPer matrix (specimen BZ70); scale bar 10μm.

Table 2. Silicate mineral compositions for Sao Luiz and other localities

Locality	Sao Luiz	Sao Luiz	Sao Luiz	Sao Luiz	Koffiefontein	Orroroo	Sao Luiz	Sao Luiz
Sample	BZ120C	BZ207A	BZ210B	BZ251B	A262	ORR3	BZ97	BZ115
Phase	**MgSiPvk**	**MgSiPvk**	**MgSiPvk**	**MgSiPvk**	**MgSiPvk**	**MgSiPvk**	**CaSiPvk**	**CaSiPvk**
Other inclusions	fPer	fPer + TAPP	fPer	fPer	fPer			u. incls.
Wt %								
SiO2	56.64	55.34	51.41	57.04	57.10	57.44	50.80	50.59
TiO2	0.22	0.19	0.02	0.15	0.03	0.00	0.00	0.01
Al2O3	1.23	2.74	10.04	1.33	1.16	0.50	0.11	0.08
Cr2O3	0.45	0.16	1.19	0.40	0.36	0.25	0.00	0.01
FeOt	4.63	9.00	5.14	3.80	3.33	4.42	0.08	0.16
MnO	0.16	0.30	0.93	0.14	0.11	0.11	0.04	0.02
NiO	0.01	0.03	0.02	0.00	0.02	0.13	0.00	0.00
MgO	35.39	32.11	30.21	36.25	36.90	36.31	0.09	0.14
CaO	0.04	0.06	0.65	0.06	0.12	0.73	48.71	48.49
Na2O	0.06	0.07	1.05	0.03	0.00	0.04	0.02	0.02
K2O		0.01	0.00	0.02	0.00	0.00		
Total	98.83	100.00	100.66	99.22	99.13	99.93	99.83	99.51
Cations								
Si	0.981	0.965	0.878	0.979	0.942	0.924	0.983	0.982
Ti	0.003	0.003	0.000	0.002	0.000	0.000	0.000	0.000
Al	0.025	0.056	0.202	0.027	0.023	0.010	0.003	0.002
Cr	0.006	0.002	0.016	0.005	0.005	0.003	0.000	0.000
Fet	0.067	0.131	0.073	0.055	0.048	0.063	0.001	0.003
Mn	0.002	0.004	0.013	0.002	0.002	0.002	0.001	0.000
Ni	0.000	0.000	0.000	0.000	0.000	0.002	0.000	0.000
Mg	0.913	0.834	0.769	0.927	0.942	0.924	0.002	0.004
Ca	0.001	0.001	0.012	0.001	0.002	0.013	1.010	1.008
Na	0.002	0.002	0.035	0.001	0.000	0.001	0.001	0.001
K	0.000	0.000	0.000	0.000	0.000	0.000	0.000	0.000
Total	2.000	2.000	2.000	2.000	2.000	2.000	2.000	2.000
Ferric-Ferrous								
Fe3+/Fet	0.20	0.20	0.75	0.20	0.20	0.20		
Fe3+	0.013	0.026	0.055	0.011	0.010	0.013		
Fe2+	0.054	0.105	0.018	0.044	0.038	0.051		
Wt% Fe2O3	1.03	2.00	4.28	0.84	0.74	0.98		
Wt% FeO	3.70	7.20	1.28	3.04	2.66	3.54		
Fe2+/(Fe2++Mg)	0.055	0.112	0.023	0.045	0.039	0.052		

Other inclusions refer to inclusions in the same diamond; "u. icnls." means small unknown inclusions or other inclusion lost on polishing.

Absence of a number means element not anlysed. Fet refers to total Fe.

Ferric-ferrous ratios are based on McCammon et al. (1997) with average Fe3+/Fet value taken as: 0.70 in TAPP, 0.2 in Al-poor MgSiPvk, 0.75 in Al-rich MgSiPvk.

Australia (SCOTT-SMITH *et al.*, 1984); and Sloane, USA (MOORE *et al.*, 1986; OTTER and GURNEY, 1989).

Ten of the São Luiz fPer occur in the same diamonds as silicate mineral associations itemised in Table 3; including one case (BZ205, Table 1) where 2 separate fPer inclusions occur in one diamond together with a TAPP inclusion. An association of oxide and silicate inclusions has been recorded so far from only one diamond outside São Luiz, and that is the occurrence of fPer and MgSiPvk in diamond A262 from Koffiefontein (in Table 1 and 2, data from MOORE *et al.*, 1986). Rare fPer and MgSiPvk inclusions from Orroroo were suggested as occurring together but were not taken from the same diamond (SCOTT-SMITH *et al.*, 1984).

All fPer are reasonably pure Mg-Fe oxide compositions (Table 1). SiO_2, TiO_2, Al_2O_3, CaO, and K_2O, are all <0.25 wt%. Other minor elements typically occur in amounts of <1.5 oxide wt%, with: Cr_2O_3 0.0 to 1.4% (excepting a value of 2.6% in inclusion BZ205C); MnO 0.1 to 0.8%; NiO 0.1 to 1.6%; Na_2O 0.00 to 1.2%.

In contrast to the restricted variation of minor elements, the range in MgO to FeO is extremely wide, although the majority of inclusions are magnesian. The São Luiz fPer have a range of $Fe^{2+}/(Fe^{2+} + Mg)$ of 0.16 to 0.64; while those from other localities recorded in the literature are restricted to the range 0.11 to 0.14, with the exception of one extreme specimen from Monastery with $Fe^{2+}/(Fe^{2+} + Mg)$ of 0.88 (MOORE *et al.*, 1986). Mössbauer spectroscopic analysis (McCAMMON *et al.*, 1997) of five of the São Luiz fPer show extremely low Fe^{3+}/Fe^t ratios of 0 to 7%. These values include Mössbauer analyses on the two most Fe-rich specimens,

Sao Luiz BZ116B CaSiPvk fPer	Sao Luiz BZ119 CaSiPvk u. incls.	Sao Luiz BZ252 CaSiPvk	Sao Luiz BZ103 Sti(SiO2) fPer	Sao Luiz BZ205A TAPP 2 fPer	Sao Luiz BZ206B TAPP fPer	Sao Luiz BZ207A TAPP fPer+ MgSiPvk	Sao Luiz BZ238A TAPP fPer	Sao Luiz BZ244B TAPP
52.01	51.03	51.18	99.26	42.54	42.43	39.56	41.41	42.12
0.05	0.02	0.06	0.01	0.02	0.01	4.20	0.03	0.06
0.05	0.07	0.07	0.04	23.88	23.48	20.16	23.33	23.83
0.01	0.01	0.03	0.01	2.47	2.22	1.39	2.99	2.80
0.08	0.04	0.16	0.07	4.96	4.64	9.41	4.98	4.60
0.00	0.04	0.06	0.01	0.84	0.47	0.25	0.92	0.96
		0.02		0.01	0.07	0.03	0.01	0.01
0.46	0.06	0.14	0.02	25.43	26.66	24.85	24.95	25.63
46.94	45.75	48.43	0.01	0.11	0.12	0.03	0.13	0.09
0.04	0.02	0.01	0.00	0.16	0.15	0.03	0.16	0.09
0.00	0.00	0.02	0.00	0.00	0.01	0.00	0.02	0.00
99.64	97.04	100.18	99.43	100.44	100.24	99.91	98.93	100.19
1.008	1.017	0.987	0.998	2.937	2.918	2.806	2.908	2.915
0.001	0.000	0.001	0.000	0.001	0.001	0.224	0.002	0.003
0.001	0.002	0.002	0.000	1.943	1.903	1.685	1.931	1.944
0.000	0.000	0.000	0.000	0.135	0.121	0.078	0.166	0.153
0.001	0.001	0.003	0.001	0.287	0.267	0.558	0.292	0.266
0.000	0.001	0.001	0.000	0.049	0.027	0.015	0.055	0.056
0.000	0.000	0.000		0.001	0.004	0.002	0.001	0.001
0.013	0.002	0.004	0.000	2.616	2.732	2.627	2.612	2.644
0.974	0.977	1.001	0.000	0.008	0.009	0.002	0.010	0.007
0.002	0.001	0.000	0.000	0.022	0.019	0.004	0.022	0.012
0.000	0.000	0.000	0.000	0.000	0.000	0.000	0.002	0.000
2.000	2.000	2.000	1.000	8.000	8.000	8.000	8.000	8.000
				0.70	0.70	0.70	0.74	0.70
				0.201	0.187	0.391	0.216	0.186
				0.086	0.080	0.167	0.076	0.080
				3.86	3.61	7.32	4.10	3.58
				1.49	1.39	2.82	1.29	1.38
				0.032	0.028	0.060	0.028	0.029

as well as Mg-rich and intermediate compositions, and suggest that Fe^{3+}/Fe^t is consistently low. The Fe^{3+}/Fe^t content of $(Mg,Fe)O$ phases is related to the solid solution of the spinel end members, magnesioferrite to magnetite ($MgO{\cdot}Fe_2O_3$ to $FeO{\cdot}Fe_2O_3$), and the restriction of such solid solution at very high pressures is consistent with experimental data (MCCAMMON et al., 1995 and 1998; see following subsection).

Examination of the variation in minor element compositions in conjunction with $Fe^{2+}/(Fe^{2+} + Mg)$ of the fPer reveals few systematic variations. The most conspicuous relationship is shown by Ni, which tends to increase as Mg increases (Fig. 1). There is also a tendency for Cr to increase with Mg in the São Luiz samples, and this may be seen in Fig. 1 if one excludes samples with $Fe^{2+}/(Fe^{2+} + Mg) < 0.17$, since most of these samples do not come from São Luiz.

SEM-TEM data on magnesioferrite-magnetite in fPer. Back-scattered electron (BSE) images made by SEM for maximum atomic number contrast (LLOYD, 1987) on fPer inclusions from São Luiz, indicate that some contain very small elongate bodies, which have a high back-scatter intensity. These bodies, illustrated in Fig. 2, are typically around 1 to $3\,\mu m$ in length and $<0.4\,\mu m$ wide, and sometimes appear to be linked together in chains which may show rough alignments. Their features are possibly the product of nucleation of material in dislocation arrays. In one case (BZ67) the tiny elongate bodies appear to have coalesced into sinuous linear arrays, which potentially represent subgrain walls.

Chemical analysis of these tiny inclusions is difficult. Scanning of small areas on the SEM shows that inclusion-rich areas have slightly higher $Fe^t/(Mg + Fe^t)$ than inclusion-poor areas. TEM investigation of specimen BZ67 shows that the elongate bodies have the crystal structure of $MgO{\cdot}Fe_2O_3$ to $FeO{\cdot}Fe_2O_3$ (magnesioferrite to magnetite) spinel solid solutions. Chemical analysis by TEM of individual inclusions and by SEM of the sinuous linear arrays in BZ67

Table 3. Lower Mantle Mineral Associations in Sao Luiz diamonds.

Mineral association	Approximate composition	No. found	$Fe^{2+}/(Fe^{2+}+Mg)$ of associated fPer
fPer	$(Mg,Fe)O$	14	0.14 to 0.62
CaSiPvk	$CaSiO_3$	4	
TAPP	$(Mg,Fe)_3Al_2Si_3O_{12}$	1	
fPer + MgSiPvk (low-Al)	$(Mg,Fe)O + (Mg,Fe)SiO_3$	2	0.15 to 0.30
fPer + MgSiPvk (high-Al)	$(Mg,Fe)O + (Mg,Fe)_{0.9}Al_{0.2}Si_{0.9}O_3$	1	0.18
fPer + CaSiPvk	$(Mg,Fe)O + CaSiO_3$	1	0.19
fPer + Sti	$(Mg,Fe)O + SiO_2$	1	0.30
fPer + TAPP	$(Mg,Fe)O + (Mg,Fe)_3Al_2Si_3O_{12}$	3	0.17 to 0.30
fPer + MgSiPvk + +TAPP	$(Mg,Fe)O + (Mg,Fe)SiO_3 + (Mg,Fe)_3Al_2Si_3O_{12}$	1	0.30

fPer - ferropericlase; MgSiPvk - MgSi perovskite; CaSiPvk - CaSi perovskite; Sti - stishovite;
TAPP - phase with almandine-pyrope garnet composition (pyrope-rich).

strongly suggests >95% of the magnesio-ferrite ($MgO \cdot Fe_2O_3$) molecule.

Approximately a quarter of the fPer contain magnesioferrite inclusions, but their occurrence shows no obvious correlation with the bulk composition of the fPer, and in particular with $Fe^{2+}/(Mg + Fe^{2+})$ or $Fe^{3+}/(Fe^{2+} + Fe^{3+})$ ratios. Their appearance suggests decoration of dislocations and it appears possible that their formation has been partly controlled by kinetic dislocation controls on nucleation as well as by chemical, P–T, or oxygen fugacity conditions. From the viewpoint of phase equilibria, little information is available on the MgO-FeO-Fe_2O_3 system at lower mantle pressures. Solid solution of high-pressure phases of $MgO \cdot Fe_2O_3$-$FeO \cdot Fe_2O_3$ in $(Mg,Fe)O$ is believed to be very restricted even at high fO_2 (MCCAMMON et al., 1995 and 1998), and the available phase data suggests that the limited exsolution described above might result from: increasing pressure, or decreasing temperature, or increasing fO_2. Of these, temperature decrease seems the more likely cause of exsolution, since the late pressure changes affecting the included minerals are more likely to be decreasing rather than increasing, and fO_2 change is unlikely to affect the inclusions after encapsulation in diamond. However, the temperature effect on exsolution would probably have to have occurred in a thermal boundary layer of the mantle convection system, because temperature changes in the rising limbs of the convective system would only be adiabatic and their effect on the phase equilibria would likely be offset by the much more substantial pressure changes occurring during upward flow (HARTE et al., 1998).

MgSiPvk compositions

Excluding BZ210B, the major-minor element compositions of these mineral grains are relatively unremarkable. They are Mg-rich, with Al_2O_3 (up to 2.7 wt%) and Cr_2O_3 (up to 0.5 wt%) as the principal components in addition to the $(Mg,Fe)SiO_3$ formula units (Table 2). The BZ210B composition shows a distinctive 10.0 wt% Al_2O_3, equivalent to 0.2 cations per $(Mg,Fe)SiO_3$ formula unit, and this specimen is referred to as *high-Al MgSiPvk* in Table 3 and below, in distinction to the other, *low-Al MgSiPvk*, compositions. Na contents are small for low-Al MgSiPvk, and Na is usually lower in MgSiPvk than that in associated fPer (Tables 1 and 2). The high-Al MgSiPvk, BZ210B, shows distinctly higher values of Cr, Mn, Ca and Na than the other MgSiPvk inclusions.

Mössbauer spectroscopy (MCCAMMON et al., 1997), has shown a low-Al MgSiPvk (BZ251) to have Fe^{3+}/Fe^t of 20%. This is reasonably similar to the value of 12% quoted by FEI et al. (1996) for experimental data. In contrast the high-Al specimen (BZ210) has Fe^{3+}/Fe^t of 75%. On the usual basis of

Table 4. Partition coefficients for associated phases

(a) Data for MgSiPvk/fPer

Symbolism	Partition ratios MgSiPvk/fPer	BZ207	BZ251	A262	ORR	Average for low-Al MgSiPvk	BZ210 high-Al MgSiPvk
$D_{Fe2+}^{MgSiPvk/fPer}$	$Fe^{2+}/(Fe^{2+}+Mg)$	0.37	0.31	0.32	0.39	0.34	0.13
$D_{Fet}^{MgSiPvk/fPer}$	$Fe^t/(Fe^t+Mg)$	0.43	0.37	0.40	0.47	0.41	0.42
$D_{Fe2+*}^{MgSiPvk/fPer}$	Fe^{2+} cations	0.36	0.30	0.32	0.38	0.34	0.11
$D_{Fe3+*}^{MgSiPvk/fPer}$	Fe^{3+} cations	4.35	3.69	3.90	4.62	4.14	15.75
$D_{Mn*}^{MgSiPvk/fPer}$	Mn cations	1.48	1.45	1.34	1.63	1.48	7.09
$D_{Ni*}^{MgSiPvk/fPer}$	Ni cations	0.06		0.04	0.26	0.12	0.03
$D_{Ca*}^{MgSiPvk/fPer}$	Ca cations	19.32	6.85			13.08	216.21
$D_{Na*}^{MgSiPvk/fPer}$	Na cations	1.09	0.38			0.74	2.70
$D_{Ti*}^{MgSiPvk/fPer}$	Ti cations	21.36	34.25			27.81	7.13
$D_{Cr*}^{MgSiPvk/fPer}$	Cr cations	0.63	2.68	1.46	2.95	1.93	2.00

(b) Data for TAPP/fPer

Symbolism	Partition ratios TAPP/fPer	BZ205	BZ206	BZ207	BZ238	Average for TAPP
$D_{Fe2+}^{TAPP/fPer}$	$Fe^{2+}/(Fe^{2+}+Mg)$	0.18	0.16	0.20	0.17	0.18
$D_{Fet}^{TAPP/fPer}$	$Fe^t/(Fe^t+Mg)$	0.53	0.51	0.62	0.58	0.56
$D_{Fe2+*}^{TAPP/fPer}$	Fe^{2+} cations	0.16	0.16	0.19	0.15	0.17
$D_{Fe3+*}^{TAPP/fPer}$	Fe^{3+} cations	18.64	17.79	21.61	21.39	19.86
$D_{Mn*}^{TAPP/fPer}$	Mn cations	7.18	3.99	1.68	7.82	5.17
$D_{Ni*}^{TAPP/fPer}$	Ni cations	0.03	0.17	0.10	0.02	0.08
$D_{Ca*}^{TAPP/fPer}$	Ca cations	20.51	82.73	12.86		38.70
$D_{Na*}^{TAPP/fPer}$	Na cations	0.99	0.35	0.57	4.08	1.50
$D_{Ti*}^{TAPP/fPer}$	Ti cations	3.72	1.73	633.61	2.30	2.58[#]
$D_{Cr*}^{TAPP/fPer}$	Cr cations	9.55	4.73	7.69	13.87	8.96

* - indicate molar partition coefficients (Beattie et al., 1993) calculated as ratio of given cation to total cations (R) per formula unit.
Formula units: $RSiO_3$ for MgSiPvk, RO for fPer, $R_{1.66}SiO_4$ for TAPP.
[#] - average calculated without BZ207.

Al-Fe^{3+} substitution relationships in silicate structures, this high Fe^{3+} content may be linked with the high Al content (WOOD and RUBIE, 1996, MCCAMMON et al., 1997). In the high-Al MgSiPvk, the 0.20 cations of Al and the 0.06 of Fe^{3+} per formula unit (Table 2) exceed those necessary (0.12 cations) to complete the Si, 6-fold coordinated site. Thus solid solution of an $Al^{[12]}Al^{[6]}O_3$ perovskite molecule, with Al in [12]-fold and [6]-fold coordination (WOOD and RUBIE, 1996) is indicated, together with some further substitution of Fe^{3+} and Cr for Al. The stoichiometry of BZ210 alone does not indicate how Al, Cr and Fe^{3+} should be distributed between the [12]- and [6]-fold coordinated sites of the perovskite structure. However, computer simulation studies (RICHMOND and BRODHOLT, 1998) suggest preferential substitution of Fe^{3+} into an Mg 12-fold site, charge balanced by Al substitution into an adjacent Si site. Further discussion on the Fe^{3+}/Fe^t and $Fe^{2+}/(Fe^{2+} + Mg)$ ratios in MgSiPvk are given below and in discussion of Fe/Mg partition coefficients.

Associated MgSiPvk and fPer which appear to be in equilibrium (see section on Fe/Mg partitioning), provide data on minor element partitioning between the two phases. The data are summarised in Table 4 and show reasonable consistency between inclusion

pairs from different diamonds. Ni markedly partitions in favour of fPer, whilst Ti and Ca decidedly favour MgSiPvk. Cr, Mn and Na atoms show weak preferences for either MgSiPvk or fPer, except for a high Mn value in high-Al MgSiPvk. These data for natural minerals are broadly similar to experimental data on Ni, Cr and Mn partitoning by KESSON and FITZGERALD (1991), but detailed comparison is limited by the restricted extent of the analytical data for the experimental charges and the limited number of natural samples. Average partition coefficients for the natural samples are compiled in Table 4. In view of the restricted number of samples and their limited composition range, a straightforward numerical average value is given in Table 4, and any samples with abundances below detection limits are ignored. Comparison of low-Al and high-Al MgSiPvk in Table 4 shows that high-Al MgSiPvk has lower partition coefficients for Fe^{2+} and Ti, but higher values for Fe^{3+}, Mn and Ca.

TAPP compositions

The TAPP phase occurs as apple green inclusions, 30 to 100 μm across, which were initially identified as a garnet (HARTE and HARRIS, 1994) on the basis of them having chemical stoichiometry fitting garnet ($R_3^{2+}R_2^{3+}Si_3O_{12}$—where R^{2+} cations are in a distorted [8]-fold coordinated site and R^{3+} in [6]-fold coordination). Crystallographic studies (HARRIS et al., 1997) have shown a markedly tetragonal structure ($a = 6.526$ Å and $c = 18.182$ Å) distinct to garnet, with three rather than two types of cation sites in addition to two Si sites. The tetragonal structure may be represented by the formula $M_1^aM_2^bM_2^cSi_3O_{12}$ (where M^a is a capped [4]-fold site, while M^b and M^c are [6]-fold sites), where M^a and M^c take cations equivalent to the R^{2+} site of garnet. Because of the close similarity of TAPP and garnet compositions and the widespread occurrence of garnet in the upper mantle, we shall often compare TAPP compositions and phase relations with those of garnet. This is also appropriate in view of the fact that TAPP has not yet been synthesised at high pressure, and although it is believed to be a primary phase, it cannot be discounted as a depressurisation product of an original high-pressure phase such as a garnet (HARRIS et al., 1997).

On the basis of the electron microprobe analysis, calculating all Fe as FeO^t, then TAPP compositions are very close to those of a pyrope-rich ($Mg,Fe)_3Al_2Si_3O_{12}$ (almandine-pyrope) garnet. It has unusually low Ca compared with both common garnet inclusions from diamonds and with garnets found in mantle xenoliths of peridotitic and eclogitic com-

positions. From the crystallographic study (HARRIS et al., 1997) and the atomic stoichiometry (Table 2), TAPP also shows no evidence of substitution of Si on the [6] sites, unlike the majoritic garnets predicted for the lower part of the upper mantle. The lack of majorite-like substitution may result from the stabilisation of the perovskite minerals (MgSiPvk and CaSiPvk) which provide a [6]-fold site for Si under lower mantle conditions as well as alternative sites for Mg/(Mg + Fe^{2+}) and Ca. The stabilisation of CaSiPvk also occurs at lower pressures than MgSiPvk, and in the lower part of the upper mantle this may cause Ca to be contained within CaSiPvk and removed from garnet-like phases before the depth of the lower/upper mantle boundary is reached. The stabilisation of MgSiPvk and solid solution of ($Mg,Fe)_3Al_2Si_3O_{12}$ garnet components in MgSiPvk proceeds in the uppermost lower mantle (see below for further discussion of phase relations).

Mössbauer analysis (McCAMMON et al., 1997) has shown that much of the Fe in TAPP occurs in the ferric form, with Fe^{3+}/Fe^t of 66% and 74% in two São Luiz inclusions. Assuming an average Fe^{3+}/Fe^t of 70% for all TAPP compositions, gives $Fe^{2+}/(Fe^{2+} + Mg)$ ratios of only 0.03 to 0.06, lower than those of low-Al MgSiPvk (Table 2); see below for further discussion. This allowance for Fe^{3+} gives totals of R^{3+} in excess of 2 in an 8 cation formula unit, and therefore in excess of the number expected for the R^{3+} site in garnet and the M^b site in TAPP. This points to substitution of Fe^{3+} on the M^a site of TAPP, and HARRIS et al. (1997) give a formula of $(Mg,Fe^{3+})[Al,Cr,Mn]_2\{Mg,Fe^{2+}\}_2Si_3O_{12}$, where ( ), [], { } indicate the M^a, M^b and M^c cation sites, and they suggest that the small deficiency in Si (Table 2) is made up by substitution of Al.

Cr is the commonest minor component of TAPP (with 0.08 to 0.17 cations out of 8 cations per formula unit - Table 2); though the abundances are low by comparison with garnets from upper mantle peridotitic xenoliths and diamonds (HARRIS et al., 1997). In one case, BZ207A, Ti is unusually high with 0.22 out of 8 cations. By comparison with the other associated phases (Tables 1, 2 and 4), it is clear that Cr and Fe^{3+} partition into TAPP rather than fPer or low-Al MgSiPvk, while Ni prefers to substitute into fPer. Mn and Ca partition into TAPP rather than fPer, but show similar preferences for TAPP and MgSiPvk in specimen BZ207. Na shows no strong preference for oxide or silicate phases.

CaSiPvk and SiO$_2$ compositions

The five CaSiO$_3$ inclusions found by electron microprobe analysis of São Luiz inclusions are remark-

ably pure; all oxides other than CaO and SiO_2 are less than 0.2wt% (Table 2), with the exception of 0.46% MgO in BZ116B. They are considered to represent primary CaSiPvk rather than wollastonite because: (a) $CaSiO_3$ is not expected in peridotite-eclogite compositions so long as Ca-rich pyroxenes and garnets are stable; (b) fPer has been found to be associated in one case.

The SiO_2 inclusion found associated with fPer in diamond BZ103 is virtually pure SiO_2 (Table 2). At the pressure conditions of the shallower part of the lower mantle this phase would have the stishovite structure.

Fe^{3+}/Fe^{2+} and Fe/Mg ratios for associated phases

The distinction of Fe^{3+} and Fe^{2+} in the mineral compositions has a marked effect on the partitioning of Fe and Mg in the fPer, MgSiPvk and TAPP compositions. This is because fPer is the most Fe-rich phase but has very low Fe^{3+}/Fe^t (ferric Fe/total Fe); whilst low-Al MgSiPvk has intermediate Fe^{3+}/Fe^t, and both of the aluminous phases, high-Al MgSiPvk and TAPP, have very high Fe^{3+}/Fe^t (Tables 1, 2 and 4; data from MCCAMMON et al., 1997). The ability of transition zone silicates to carry relatively substantial Fe^{3+} has been noted by O'NEILL et al. (1993), who also note that this does not necessarily imply high oxygen fugacity, but will have an important effect on physical properties such as electrical conductivity.

MgSiPvk and fPer associations. Figures 3a and 3b show relative partitioning of Fe^t/Mg, and Fe^{2+}/Mg, between associations of MgSiPvk and fPer in four diamonds from São Luiz and one diamond from Koffiefontein. We have also added the data for MgSiPvk and fPer from Orroroo using the average of two very similar fPer compositions reported from Orroroo (SCOTT-SMITH et al., 1984), even though the Orroroo inclusions are not in the same diamond. The $Fe^t/(Fe^t + Mg)$ parameter plotted in Fig. 3a corresponds with the Fe/(Fe + Mg) parameters of FEI et al. (1991, 1996) and WOOD and RUBIE (1996), or their parameters X_{Fe} and Fe# respectively, where Fe^{2+} and Fe^{3+} are not separated. Whether calculated with Fe^t or Fe^{2+} (Fig. 3 and Table 4), compositions from four of the diamonds (BZ251and BZ207 from São Luiz, together with the Koffiefontein and Orroroo stones) show closely similar partitioning of Fe between MgSiPvk and fPer with an average $D_{Fe}^{MgSiPvk/fPer}$ of 0.34 for $Fe^{2+}/(Fe^{2+} + Mg)$ and 0.41 for $Fe^t/(Fe^t + Mg)$. FEI et al. (Fig. 8, 1991) using experimental data for similarly magnesian compositions from several sources, show an average $D_{Fet}^{MgSiPvk/fPer}$ of ca. 0.23, and a similar value is suggested from other experimental data (GUYOT

et al., 1988; WOOD and RUBIE, 1996). KESSON and FITZGERALD (1991) give experimental data for $D_{Fet}^{MgSiPvk/fPer}$ ranging from approximately 0.2 to 0.4, but with a marked dependence on the bulk $Fe^t/(Fe^t + Mg)$, which is not evident in our limited data set or that of FEI et al. (1991).

In Figs. 3a and 3b the associated MgSiPvk-fPer mineral pair for diamond BZ120 do not appear to represent equilibrium by comparison with the other inclusion data, irrespective of whether $Fe^{2+}/(Fe^{2+} + Mg)$ or $Fe^t/(Fe^t + Mg)$ is considered. This is also indicated on the SiO_2-MgO-FeO plot of Fig. 6b, where the dotted tie-line for BZ120 is not aligned with the other MgSiPvk-fPer tie-lines.

All the above inclusion pairs involve low-Al MgSiPvk, and the situation for high-Al MgSiPvk is clearly different, as predicted from experimental data by WOOD and RUBIE (1996). In the case of high-Al MgSiPvk a much higher proportion of the Fe is present as Fe^{3+}, and on the $Fe^{2+}/(Fe^{2+} + Mg)$ plot (Fig. 3b) the BZ210 inclusion is displaced from the other inclusions and shows a $D_{Fe2+}^{MgSiPvk/fPer}$ of only 0.13 compared with the average of 0.34 for the low-Al MgSiPvk inclusion associations (excluding the aberrant BZ120). On the other hand, the Fe^t plot (Fig. 3a) shows BZ210 with a slightly higher $D_{Fet}^{MgSiPvk/fPer}$ than the other inclusions, and this increase of $Fe^t/(Fe^t + Mg)$ in the high-Al MgSiPvk is in accord with the relationships derived from experimental charges by WOOD and RUBIE (1996). However, in contrast to the WOOD and RUBIE (1996) prediction based on Fe^t, the distinction of Fe^{2+} and Fe^{3+} in the natural minerals, shows that the effect of high-Al is not so much to increase $Fe^t/(Fe^t + Mg)$ as to lower $Fe^{2+}/(Fe^{2+} + Mg)$ in the MgSiPvk (Fig. 3, Table 4). The different orientation of the BZ210 high-Al MgSiPvk tie-line, compared with other MgSiPvk-fPer tie-lines, is also apparent in Fig. 6b.

TAPP associations. Figures 3c-d and Table 4 show $Fe^t/(Fe^t + Mg)$ and $Fe^{2+}/(Fe^{2+} + Mg)$ for TAPP and fPer associations from four São Luiz diamonds. In the case of diamond BZ205 two fPer occur in the same stone, but have very different compositions and both cannot be in equilibrium with TAPP. Figures 3c and 3d show very clearly that it is fPer BZ205C that is out of equilibrium, whilst BZ205B fits in with data from the other associations. Excluding BZ205C the TAPP/fPer associations have similar $D_{Fe}^{TAPP/fPer}$ for $Fe^{2+}/(Fe^{2+} + Mg)$ and $Fe^t/(Fe^t + Mg)$, with average values of 0.18 and 0.56 respectively. The marked difference between the $Fe^{2+}/(Fe^{2+} + Mg)$ and $Fe^t/(Fe^t + Mg)$values reflects the very large proportion of Fe^t that is Fe^{3+} in TAPP.
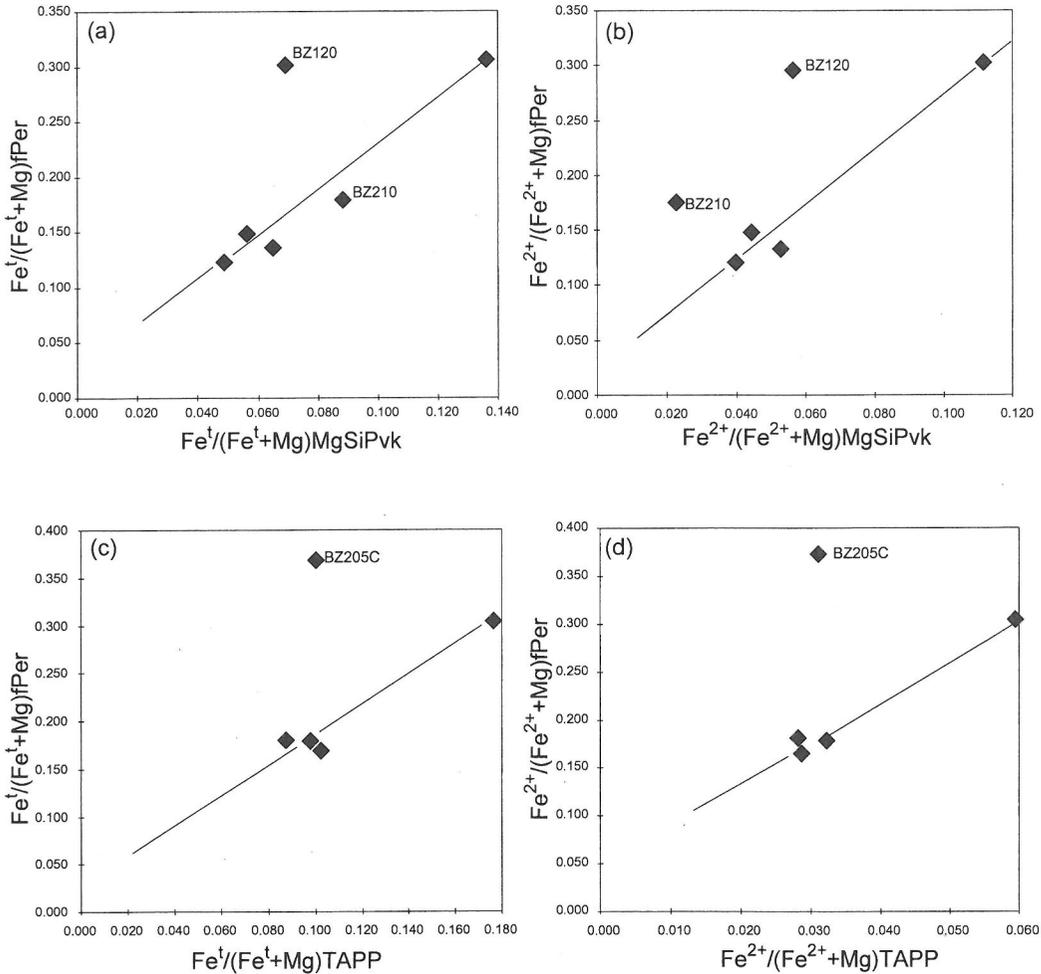
FIG. 3. Plots of $Fe^t/(Fe^t + Mg)$ and $Fe^{2+}/(Fe^{2+} + Mg)$ for associations in the same diamond of MgSiPvk with fPer, and TAPP with fPer; in atomic proportions from the data of Tables 1 and 2; where Fe^t refers to total Fe. (a) $Fe^t/(Fe^t + Mg)$ MgSiPvk vs $Fe^t/(Fe^t + Mg)$ fPer, (b) $Fe^{2+}/(Fe^{2+} + Mg)$ MgSiPvk vs $Fe^{2+}/(Fe^{2+} + Mg)$ fPer, (c) $Fe^t/(Fe^t + Mg)$ TAPP vs $Fe^t/(Fe^t + Mg)$ fPer, and (d) $Fe^{2+}/(Fe^{2+} + Mg)$ TAPP vs $Fe^{2+}/(Fe^{2+} + Mg)$ fPer. Note that for (b) and (d), the Fe^{2+} contents are based in many cases upon average values of Fe^{2+}/Fe^t for each phase using the data of MCCAMMON et al. (1997), see also Tables 1 and 2. Lines give average $D^{MgSiPvk/fPer}$ and $D^{TAPP/fPer}$, excluding mineral pairs given specimen numbers (with BZ prefix); see text for further explanation.

TRACE ELEMENT AND STABLE ISOTOPE COMPOSITIONS

Diamond characteristics

The São Luiz diamonds containing the inclusions discussed in this paper show a number of distinctive features. They are generally characterised by irregular and dodecahedral morphologies, but most particularly by a very high proportion of stones with Type II nitrogen charcteristics (WILDING, 1990; HUTCHISON, 1997), whereby nitrogen contents are at or below the

limits of detection by Fourier transform infra-red techniques (FTIR).

In addition, bulk determinations of carbon isotope composition show a tight grouping of values. WILD-ING (1990) made 5 determinations of diamonds with lower mantle minerals (including diamonds with a CaSiPvk inclusion, a SiO_2 inclusion, and BZ66 with the most Fe-rich fPer), and found $\delta^{13}C$ ranging from -4.14 to -5.15. Further data (HUTCHISON, 1997; HUTCHISON et al., 1998), including analyses of diamonds which contained MgSiPvk and TAPP inclu-

sions, have expanded this range of $\delta^{13}C$ for bulk diamonds with lower mantle associations to -3.47 to -7.88. Thus the bulk compositions are closely grouped around the -5 to -6 values typical of many diamonds, which are believed to represent typical mantle compositions (HARRIS, 1987; GURNEY, 1989).

Trace element data for included minerals

The trace element compositions of inclusions analysed by ion microprobe are given in Table 5, and a plot of average compositions is shown in Fig. 4. The small size of many of the silicate inclusions (20–50 μm), coupled with often low trace element abundances, has made it difficult to obtain good absolute and relative abundance patterns for many of the inclusions. Only CaSiPvk inclusions are the exception, and analyses of two of these inclusions show considerable similarity, with most elements showing abundances substantially above chondrite. The LREE and MREE have abundances about 200× chondrite, while those of the HREE drop progressively with decreasing ionic radius from this value to about 80× chondrite. Y and Zr abundances are ca. 90× and 50× chondritic respectively. Only K and Ba have subchondritic abundances. A most notable feature of both the CaSiPvk analyses is the presence of a small positive Eu anomaly (Table 5, Fig. 4).

The abundances of many trace elements in fPer, MgSiPvk and TAPP were near the detection limits (Table 5), and in Fig. 4 they are represented by average compositions. Given the large error of ion microprobe analyses at such abundance levels, the average values plotted in Fig. 4 have been compiled by considering individual analysis values below detection limit to be zero; where an element gave consistent values below detection limits it has been ignored in drafting Fig. 4. This means that the values of Fig. 4 must be considered as only indicative of relative concentrations amongst MgSiPvk, TAPP, and fPer, and are likely to be maxima in absolute terms. The patterns illustrated in Fig. 4 are rather 'spiky', in reflection of the low abundances, and show that fPer tends to have slightly higher abundances than the co-existing MgSiPvk and TAPP silicates. The one marked exception is a high value of Zr in the BZ207 TAPP, though this is not seen in the other TAPP analysed (Table 5). Because of this marked difference between the two TAPP's, an average value has not been plotted in Fig. 4. Distinct enrichment of TAPP in MREE and HREE is not seen; unlike garnet in the upper mantle. On crystal chemical grounds this is not surprising because REE show a close link with Ca distribution (*e.g.,* HARTE and KIRKLEY, 1997), and in the present lower mantle situation TAPP is Ca

poor, with virtually all Ca being in CaSiPvk. MgSiPvk, the most abundant phase expected in the lower mantle, has low trace element inventories irrespective of its Al content. All the phases except CaSiPvk show evidence of anomalously low Y (Fig. 4), when Y abundances are compared with the geochemically similar element, Ho.

One feature of the trace element distributions that is clearly hidden by the average values of Fig. 4, is evidence of composition variation related to $Fe^{2+}/(Fe^{2+} + Mg)$. For the silicate phases, evidence of such relations is limited by the small number of analyses and low abundances, but there are considerably more data concerning fPer. In Fig. 5 we plot fPer compositions as a function of $Fe^{2+}/(Fe^{2+} + Mg)$, for the relatively abundant elements Sr, La, Y and Zr. The diagram provides evidence of a significant drop in abundances as $Fe^{2+}/(Fe^{2+} + Mg)$ increases. Thus, the fPer associated with MgSiPvk and TAPP [with $Fe^{2+}/(Fe^{2+} + Mg)$ <0.30] show distinctly higher abundances than those of the more Fe-rich fPer. It is also interesting to note that the magnesian fPer appear to be as favoured a location for K and Ba as their associated silicates, which coincides with the relatively high contents of Na in the fPer (Table 1).

In showing the CaSiPvk as the major holder of REE, the above results for the natural assemblages show a general agreement with the experimental results of KATO *et al.* (1988, 1996) for phase assemblages involving combinations of CaSiPvk, MgSiPvk, majoritic garnet and melts. The major difference to the relationships indicated by the São Luiz analyses is that KATO *et al.* (1988, 1996) found Zr to partition somewhat preferentially into MgSiPvk compared with CaSiPvk, whilst we have found high concentrations of Zr in CaSiPvk and TAPP but not in MgSiPvk.

It is interesting to consider what values of trace element abundances in a lower mantle ultrabasic rock composition might be implied by the São Luiz data. We have therefore calculated the bulk trace element composition for a combination of São Luiz phases giving the major element (SiO_2, Al_2O_3, FeO^t, MgO and CaO) composition of pyrolite (IRIFUNE and RINGWOOD, 1987; McDONOUGH and SUN, 1995). A good approach to such a major element composition is given by 77% MgSiPvk, 16% fPer, and 7% CaSiPvk; using an average of the São Luiz compositions BZ120 and BZ210 for MgSiPvk, BZ103 and BZ116 for fPer, and Bz97 and BZ 115 fo CaSiPvk. Taking the trace element data from these same minerals in the same proportions (77% MgSiPvk, 16% fPer, and 7% CaSiPvk) yields the bulk trace element composition labelled as SLLM Pyrolite in Fig. 4. This may

Table 5. Trace element data in ppm for Sao Luiz inclusions.

| Spec no. | BZ66 | BZ67 | BZ70 | BZ73 | BZ74 | BZ103 | BZ116 | BZ120 | BZ205B | BZ206 | BZ207 | BZ210 | BZ120 | BZ207 | BZ210 | BZ206 | BZ207 | BZ297 | BZ115 |
Phase	fPer	fPer	fPer	fPer	fPer	fPer	fPer	fPer	fPer	fPer	fPer	fPer	MgSiPvk	MgSiPvk	MgSiPvk	TAPP	TAPP	CaSiPvk	CaSiPvk
K	30.400	18.100	31.200	11.800	8.510	50.100	bdl	5.540		bdl			16.400	19.000		44.050	18.400	3.280	39.600
Ba	0.067	bdl	0.027	bdl	0.026	2.386	0.008	0.039	2.000	0.024	0.192	2.030	0.039	0.211	0.044	0.630	0.151	0.926	0.160
Sr	0.122	0.199	0.407	0.164	0.149	0.239	0.748	0.332	1.450	0.759	0.467	1.740	0.064	0.305	0.234	0.379	0.165	719.00	415.250
La	0.005	bdl	0.044	bdl	bdl	0.193	0.031	0.008	0.728	0.023	0.021	0.137	0.009	0.323	0.006	0.019	0.063	80.500	29.550
Ce	0.012	bdl	0.021	bdl	bdl	0.900	0.034	0.016	0.709	0.011	0.025	0.175	0.010	1.620	0.005	0.008	0.327	262.333	140.750
Pr						bdl			0.246	bdl	0.007	0.024			bdl	0.008		37.500	20.100
Nd	0.042	bdl	bdl	bdl	bdl	0.240	0.042	0.291	0.680	0.007	bdl	0.116	bdl	0.170	bdl	0.093	0.195	184.667	115.525
Sm		bdl		bdl		0.008			0.330	0.021	0.080	bdl	bdl	0.009	bdl	0.016	0.177	51.167	37.275
Eu		bdl		bdl		0.007		0.072	0.148	bdl	0.022	bdl	bdl		0.005	0.015		22.805	19.288
Gd						bdl			0.293	bdl	bdl	0.007			bdl	0.137		62.950	45.000
Tb		bdl				bdl	bdl						bdl	0.004		0.012	bdl	6.260	5.540
Dy	0.003	bdl	bdl	bdl	bdl	bdl	bdl	0.298	0.555	bdl	0.084	0.055	bdl	bdl	bdl		bdl	42.967	36.150
Ho		bdl		bdl		0.050	bdl		0.248	0.003	bdl	0.006	0.004	0.007	0.004	0.009	bdl	6.753	5.998
Er		bdl		bdl							bdl		0.036			0.009		12.300	11.295
Tm																			
Yb		bdl		bdl		bdl	bdl		1.050	bdl	0.001	bdl			0.018	0.028		9.830	8.160
Lu						bdl			0.312	bdl			0.021	0.001	0.002		0.007	1.984	1.327
Y	0.012	0.022	0.017	0.020	0.039	0.030	0.120	0.078	0.261	0.060	0.040	0.207	0.038	0.010	0.004	0.032	0.075	141.667	130.000
Zr	0.052	0.083	0.238	0.121	0.338	0.267	1.570	0.207	0.967	0.245	0.369	1.600	3.010	2.740	0.575	1.180	783.0	172.667	87.267

bdl: below detection level; a blank means not analysed
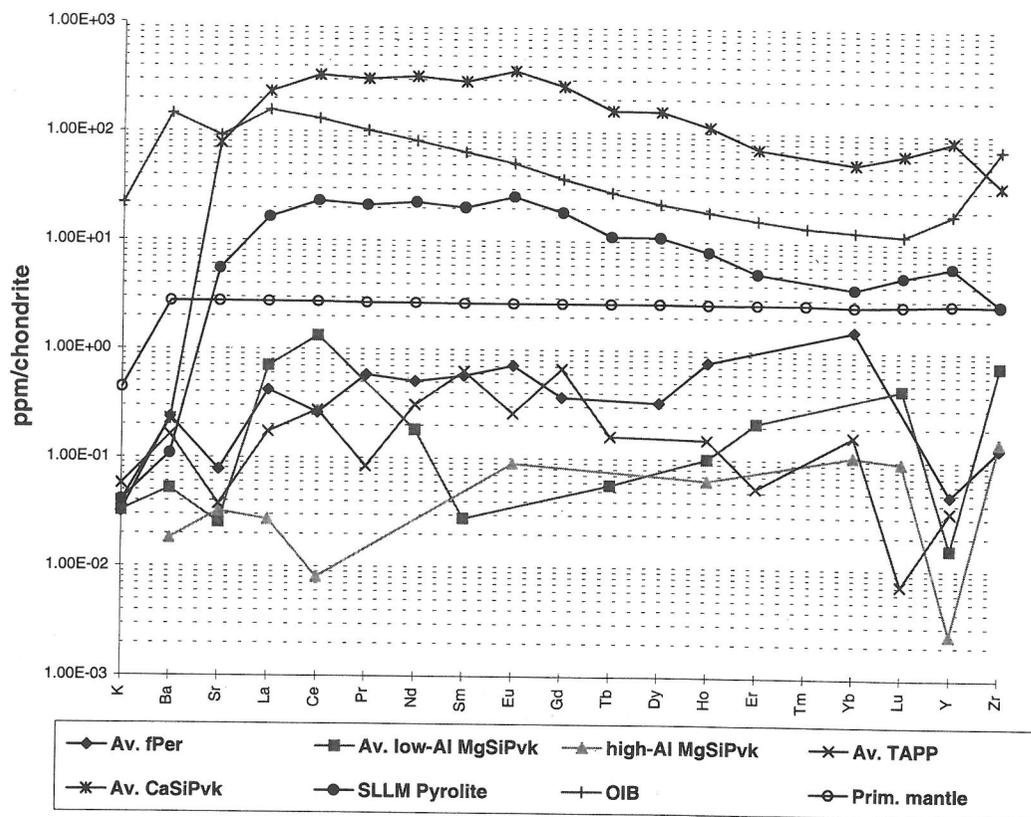
FIG. 4. Trace element abundance patterns normalised to chondrite values. The data plotted for MgSiPvk, TAPP, and fPer are average values from several São Luiz mineral inclusions (data in Table 5); average values below detection limit have been ignored. The values for SLLM pyrolite were calculated by combining data for São Luiz MgSiPvk, fPer and CaSiPvk in the ratio 77%, 16% and 7% respectively (these ratios giving a pyrolite bulk major element composition for the elements Si, Al, Fe, Mg and Ca); see text for further details. The data for primitive mantle is from MCDONOUGH and SUN (1995), the chondrite normalisation values and OIB data are from SUN and MCDONOUGH (1989).

be compared to the global estimate of primitive mantle composition based on the pyrolite model by Mc-DONOUGH and SUN (1995), which is also shown 'Prim mantle' in Fig. 4, and average OIB composition (SUN and MCDONOUGH 1989). The SLLM pyrolite estimate lies between these two, with abundances similar those of MOR basalts (SUN and MCDONOUGH 1989). Convective mixing of crustal and mantle material, as suggested in the discussion section of this paper, might therefore be responsible for the São Luiz compositions. In any situation, it is clear that the distribution and phase relationships of CaSiPvk, even when it is present in small amounts, are going to dominate trace element behaviour in the lower mantle.

Oxygen isotope composition of CaSiPvk

Oxygen isotope composition potentially may be used to assess original protolith compositions and

equilibration with normal mantle protoliths (MATTEY *et al.*, 1994; CHAZOT *et al.*, 1997). Unfortunately, reliable SIMS measurements for stable isotopes require good flat polished surfaces and calibration with a phase of closely similar composition (VALLEY *et al.*, 1998). These conditions are hard to meet for the present inclusions, because the silicates are generally less than 50 μm across and have generally been submitted to trace element analysis by ion microprobe, whilst the fPer require special standards to calibrate their wide range of Fe/(Fe + Mg). Under the circumstances only one inclusion was worthy of analysis, this being a CaSiPvk still enclosed in diamond, but which had been exposed during polishing the diamond.

Oxygen isotope analyses were made at two points on this CaSiPvk, using a wollastonite (CaSiO$_3$) of known δ^{18}O as standard. The two measurements yielded values of δ^{18}O of 4.92 and 6.95 permil with
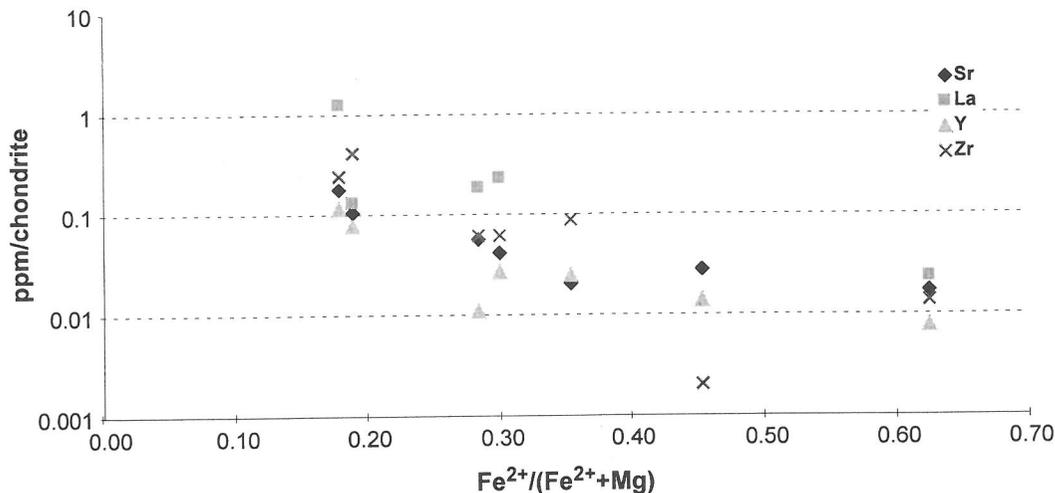
FIG. 5. Abundances of selected trace elements in fPer inclusions, plotted against $Fe^{2+}/(Fe^{2+} + Mg)$. Data for all fPer inclusions given in Table 4 are included; where several fPer have the same $Fe^{2+}/(Fe^{2+} + Mg)$ their values have been averaged, thus values given at 0.18 and 0.30 $Fe^{2+}/(Fe^{2+} + Mg)$ are respectively the average of three and four inclusions.

a standard error of *ca.* ± 1 permil. Within error, these data are very close to the estimated mantle signature of near *ca.*5.4 permil (MATTEY *et al.*, 1994; CHAZOT *et al.*, 1997), and thereby support a mantle origin for the oxygen of the inclusion. Unfortunately, the results do not descriminate as to whether the oxygen has always been within the mantle, or whether its history might have included forming part of an erupted crustal basalt at some time.

PHASE RELATIONSHIPS AND MINERAL FACIES IN THE UPPERMOST LOWER MANTLE

Phase compositions of assemblage SiO₂-fPer-MgSiPvk in the system SiO₂-MgO-FeO

Experimental studies (*e.g.,* LIU, 1975; YAGI *et al.*, 1979; ITO and TAKAHASHI, 1989; FEI *et al.*, 1991, 1996) at ultrahigh pressures have shown that Mg- and Fe-perovskites along the join MgSiO₃-FeSiO₃ have a stability range restricted to relatively Mg-rich compositions (referred to here as MgSiPvk). In more Fe-rich bulk compositions perovskite is replaced by the mineral pair SiO₂-fPer (or magnesiowüstite instead of fPer in Fe-rich assemblages). The phase compositions of the limiting assemblage in which MgSiPvk, fPer and SiO₂ co-exist is therefore of crucial importance in determining the limits on MgSiPvk and SiO₂ occurrence in the rock compositions of lower mantle, and has implications for the physical as well as chemical characteristics of the lower mantle (*e.g.,* ITO and TAKAHASHI, 1989; FEI *et al.*, 1996).

The São Luiz inclusions show a series of associa-

tions of MgSiPvk and fPer, and also one association of an SiO₂ phase with fPer, which may be used to help define the limiting SiO₂-fPer-MgSiPvk phase field. At given pressure and temperature conditions then the most Fe-rich MgSiPvk possible should co-exist with a fPer that can also co-exist with SiO₂ (Fig. 6). In fact the inclusion associations fit this relationship extremely well. The most Fe-rich MgSiPvk, in diamond BZ207, has $Fe^{2+}/(Fe^{2+} + Mg)$ of 0.11 and is associated with an fPer having $Fe^{2+}/(Fe^{2+} + Mg)$ of 0.30; whilst in diamond BZ103 an fPer associated with SiO₂ also has a $Fe^{2+}/(Fe^{2+} + Mg)$ of 0.30. Combining these relationships, the position of the limiting SiO₂-fPer-MgSiPvk assemblage is shown in Fig. 6.

Comparison with experimental data shows general good agreement with this estimate of the limiting (most Fe-rich composition) for MgSiPvk (ITO and TAKAHASHI, 1989; FEI *et al.*, 1991, 1996). For likely conditions in the uppermost lower mantle of ca. 25 GPa and 1600°C, ITO and TAKAHASHI (1989) determined the limiting composition for MgSiPvk in equilibrium with SiO₂ and fPer as having 0.11 Fe/(Fe + Mg), which is very close to the value from the São Luiz natural assemblages of $Fe^t/(Fe^t + Mg)$ of 0.14. However, their estimate of the composition of the co-existing fPer at Fe/(Fe + Mg) of 0.58 is much higher than our value of 0.30 and indicates a lower $D_{Fet}^{MgSiPvk/fPer}$. Fe^{3+}/Fe^t is not recorded for the Ito and Takahashi data. At similar experimental conditions of 26 GPa and 1600 °C, FEI *et al.* (1996) estimated
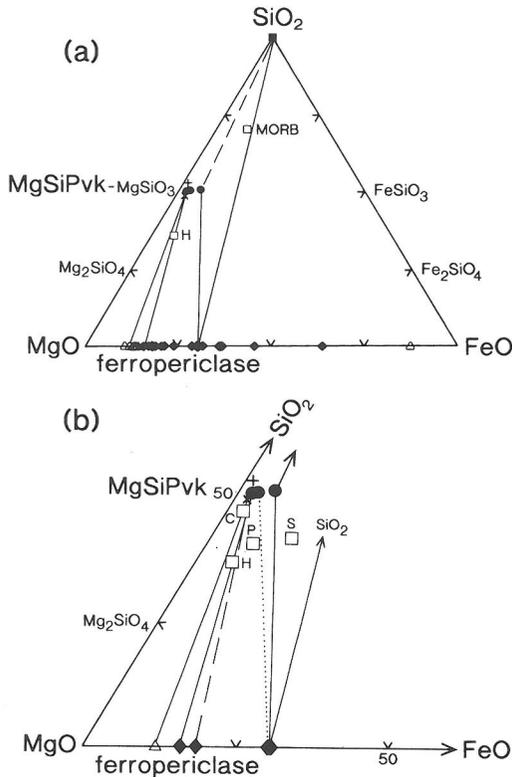
FIG. 6. Phase compositions and relations in SiO_2-MgO-FeO (molecular proportions). (a) Compositions of (Mg,Fe)O (ferropericlase-magnesiowüstite) inclusions from São Luiz (solid diamond symbols) and other localities (open triangles), together with associated (Mg,Fe)SiO_3 (MgSiPvk) and SiO_2 inclusions occurring in the same diamond as a ferropericlase (fPer) grain. Solid circles are MgSiPvk (with low Al_2O_3) from São Luiz, x is MgSiPvk (with low Al_2O_3) from Koffiefontein; cross is a high Al_2O_3 grain from São Luiz; solid square is a SiO_2 inclusion from São Luiz. The tie-lines connect mineral inclusions in the same diamond and are believed to represent compositions in equilibrium with low Al_2O_3 MgSiPvk solid solutions. The dashed line joining MgSiPvk with SiO_2 is not based on actual associated inclusions, but is put in to indicate the expected position of the MgSiPvk-fPer-SiO_2 three-phase field. Open squares show positions in SiO_2-MgO-FeO compositional space of primitive MORB and depleted oceanic harzburgite (H) compositions (IRIFUNE and RINGWOOD, 1987). (b) MgO-rich portion of SiO_2-MgO-FeO triangle showing inclusion compositions associated in one diamond. Solid tie-lines join compositions believed to be in equilibrium with low Al_2O_3 MgSiPvk (see diagram a); dashed tie-line joins associated high Al_2O_3 MgSiPvk and fPer; dotted tie-line joins MgSiPvk and fPer occurring in one diamond but not believed to be in equilibrium (see text). Representative bulk compositions are: H—depleted harzburgite; P—pyrolite (IRIFUNE and RINGWOOD, 1987); C—chondritic mantle composition and S—solar mantle composition (ANDERSON, 1989), plotted with all Fe as FeO.

the maximum Fe of the limiting MgSiPvk composition as 0.10 to 0.13 Fe/(Fe + Mg). FEI *et al.* (1996) estimated Fe^{3+}/Fe^t as 0.12 in their experimental charges, thus giving $Fe^{2+}/(Fe^{2+} + Mg)$ of 0.9 to 0.12, which compares well with 0.11 from our natural data.

Phase compositions of assemblage SiO_2-fPer-MgSiPvk-TAPP

The diamond giving the Fe-rich association of MgSiPvk and fPer used above to define the position of the SiO_2-fPer-MgSiPvk phase field, also contained TAPP. Since the MgSiPvk and TAPP are actually in contact in this diamond, it further allows definition of the SiO_2-fPer-MgSiPvk-TAPP phase field. Relations between fPer, MgSiPvk and TAPP are further illustrated in Fig. 7 and the three-phase assemblage from diamond BZ207 is indicated. Because of the disequilibrium noted above, only the fPer BZ205B composition, and not that of BZ205C, is connected to the TAPP composition by a tie-line.

The left to right plotting positions of Fig. 7 are again based on $Fe^{2+}/(Fe^{2+} + Mg)$ mineral compositions and leave out Fe^{3+}. The high $Fe^{2+}/(Fe^{2+} + Mg)$ of the fPer compared to both of the ferromagnesian silicates is very marked, as well as the fact that MgSiPvk has a higher $Fe^{2+}/(Fe^{2+} + Mg)$ than TAPP. This is the inverse of what is known for phases of equivalent composition (orthopyroxene and garnet) in the upper mantle, and is the inverse of what is often assumed for garnet-like phases in the lower mantle (*e.g.,* WOOD and RUBIE, 1996). Note that the high-Al MgSiPvk shows similarly low $Fe^{2+}/(Fe^{2+} + Mg)$ to TAPP, and both have high Fe^{3+}/Fe^t.

TAPP phase relations

The nature of the phase or phases carrying Al in the lower mantle has been a matter of uncertainty from experimental data for some time (*e.g.,* ITO and TAKAHASHI, 1987; IRIFUNE and RINGWOOD, 1993; AHMED-ZAID and MADON, 1995). This uncertainty remains, but in one respect there is now a wide consensus (*e.g.,* O'NEILL and JEANLOZ, 1994; KESSON *et al.*, 1995; IRIFUNE *et al.*, 1996; HIROSE *et al.*, 1999) that majoritic garnet, although stable at the 660 km discontinuity, becomes unstable with increasing depth, and this instability is accompanied by Al becoming substantially incorporated in MgSiPvk solid solution.

In the first instance, a difference between the São Luiz inclusions and the experimental relations, is given by the crystallographic structure of TAPP, which has not been reported from experimental in-
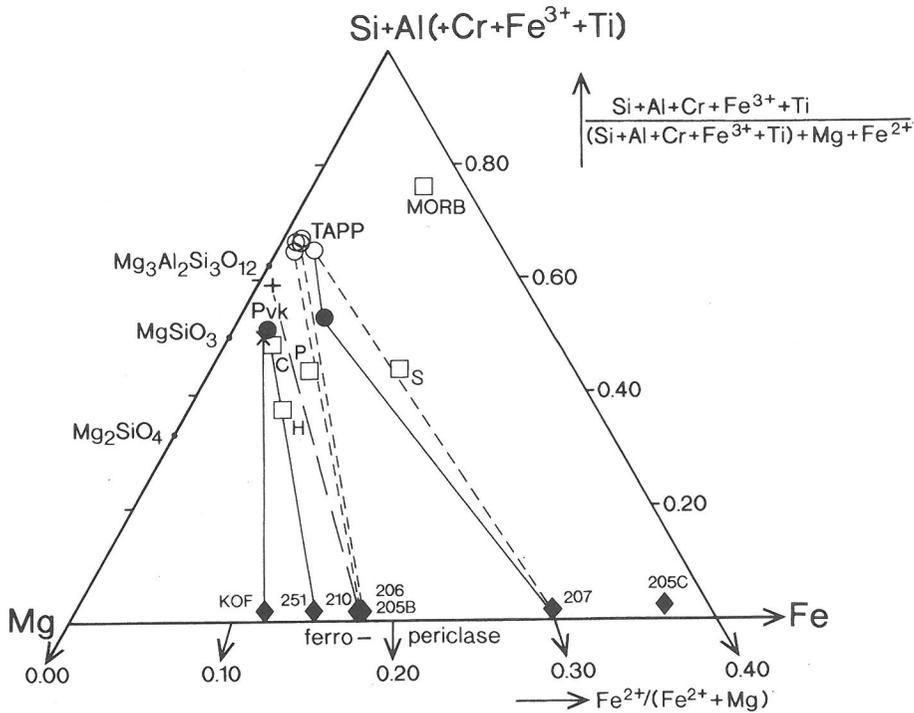
FIG. 7. Phase compositions and relations of fPer, MgSiPvk and TAPP in Mg-Fe-(Si+Al) space. (Si+Al) apex calculated as mineral cations ratio [(Si + Al + Cr + Fe^{3+} + Ti)/(Si + Al + Cr + Fe^{3+} + Ti) + Mg + Fe^{2+}], and Mg:Fe ratios as cations $Fe^{2+}/(Fe^{2+} + Mg)$ - as in the manner of the projection of THOMPSON (1957). Tie-lines join inclusions associated within one diamond: solid lines for low-Al MgSiPvk and fPer, long dashed lines for high-Al MgSiPvk and fPer; short dashed lines for TAPP and fPer. Only compatible TAPP-fPer tie-lines shown (diamonds BZ205, BZ206 and BZ207); no tie-line is shown to the fPer BZ205C composition because this is incompatible with the other data (see text and Fig. 3). Bulk compositions for: H—depleted harzburgite; P—pyrolite; C—chondritic mantle; S—solar mantle; and MORB—basalt (see also Fig. 6) are plotted as atomic proportions with all Fe calculated as Fe^{2+}.

vestigations and is distinct to garnet, even though TAPP compositions are similar to those of pyrope-almandine garnets. Although the major evidence indicates TAPP to be primary phase, its density in particular opens the possibilty that it is of decompression origin (HARRIS et al., 1997). Thus it is possible that TAPP actually represents a garnet structure under lower mantle conditions.

Although TAPP has garnet-like compositions, it also differs from the garnets synthesised experimentally, in that it shows no evidence of the majorite substitution of Si in place of Al. This substitution is regarded as typical of experimental run products at lower mantle conditions, in continuance of the widespread stability of majoritic garnet in the deeper part of the upper mantle. However, experimental work also shows restriction of the distribution and composition of such garnet as a consequence of the stabilisation of CaSiPvk in the lowermost upper mantle and MgSiPvk at the upper-lower mantle boundary. In

effect the progressive reduction in the composition field of garnet with increasing depth, coupled with the extending substitution of Al into MgSiPvk, leads to the eventual instability of all garnet at depths somewhere near 730 km (27 GPa) or a little deeper (O'NEILL and JEANLOZ, 1994; KESSON et al., 1995; MIYAJIMA et al., 1996; IRIFUNE et al., 1996; HIROSE et al., 1999). The precise depth interval of co-existence of 'garnet' and MgSiPvk, will clearly depend on the precise mineral compositions involved (and therefore the rock bulk composition).

The essence of these relationships may be seen in the $MgSiO_3$-Al_2O_3 binary system, and Fig. 8a shows the recent summary of relationships based on experimental data by IRIFUNE et al. (1996). It should be noted that the formation of ilmenite-structured $MgSiO_3$ just before perovskite-structured $MgSiO_3$ in this diagram depends critically on the exact pressure and temperature gradient across the upper-lower mantle boundary, and is not critical to the present discussion.
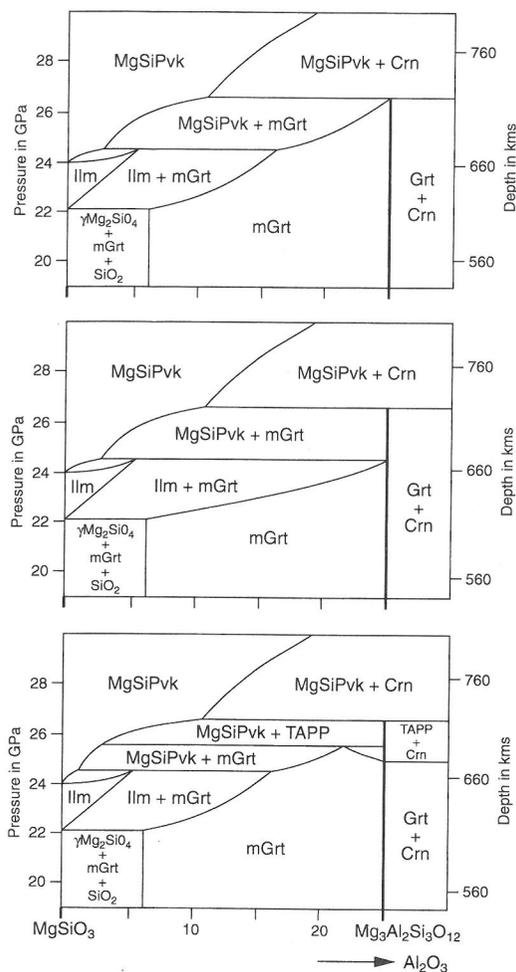
FIG. 8. Phase relations in the MgSiO₃-Al₂O₃ system at pressure and temperature conditions close to the upper-lower mantle boundary. MgSiPvk is perovskite structured MgSiO₃, Ilm is ilmenite structured MgSiO₃, Grt is pyrope (Mg₃Al₂Si₃O₁₂) garnet, mGrt is pyrope garnet with majoritic substitution, Crn is corundum, TAPP is tetragonal phase with pyrope chemical composition. (a) top: Relationships at 1500°C, as determined experimentally by IRIFUNE *et al.* (1996); (b) centre: Modification of (a) for occurrence of nonmajoritic garnet in association with MgSiPvk; and (c) bottom: Modification of (a) for occurrence of TAPP, with the chemical composition of a non-majoritic garnet but a crystal structure distinct to garnet.

The IRIFUNE *et al.* (1996) diagram (Fig. 8a) shows well that with increasing depth: (a) the composition field of majoritic garnet is dramatically restricted towards pyrope compositions over a range of ca 4.5 GPa, (b) the composition field of MgSiPvk expands, and (c) pyrope garnet becomes unstable near 27 GPa.

In Figs. 8b and 8c we show that relatively little modification of the experimental relationships of IRI-

FUNE *et al.* (1996) is necessary in order to accommodate the features shown by the São Luiz inclusions. Taking the simplest modification, which would assume that TAPP actually represents a decompressed lower mantle garnet, then the São Luiz assemblages may be accommodated by restricting majoritic garnet substitutions to lower pressures. In Fig. 8b this is done by placing the limit of majoritic garnet at same pressure as that of MgSiPvk stabilisation. On the other hand, if TAPP is truly a lower mantle phase, then a separate phase field must exist for it at pressures above those of garnets. Within the main confines imposed by the experimental data in Fig. 8a, a stability field for TAPP may be inserted as shown in Fig. 8c. In constructing Fig. 8c we have used the natural inclusion compositions to modify the limits of Al solid solution in MgSiPvk shown in Fig. 8a, but the change is not substantial within the limits of determination of experimental mineral compositions (IRIFUNE, 1994; IRIFUNE *et al.*, 1996).

In both Figs. 8b and 8c the lowest pressure compositions of co-existing MgSiPvk and garnet or TAPP are based on the inclusion compositions of MgSiPvk and TAPP in contact in diamond BZ207. The relationships of Fig. 8 also show that the high-Al MgSiPvk composition of inclusion BZ210B, could be formed at the higher pressure conditions where solid solution of Al in MgSiPvk becomes substantial. Thus the composition of MgSiPvk BZ210B may either co-exist with corundum at pressures just above the limit of garnet-TAPP stability field, or fall completely within the aluminous MgSiPvk phase field at still higher pressures. It is interesting to note that a corundum inclusion has been reported from the São Luiz inclusion suite by WATT *et al.* (1994), but it did not occur in association with fPer or the silicate phases reported herein, and its potential significance as a lower mantle inclusion was not considered. Further data on Al₂O₃-bearing associations is given by HUTCHISON (1997) and will be presented elsewhere (HUTCHISON *et al.*, in prep.).

Irrespective of the detailed differences in the phase relationships portrayed in Fig. 8, the stability field for garnet and/or TAPP must be very small compared to the whole range of pressures of the lower mantle. The experimental data of IRIFUNE (1994) and IRIFUNE *et al.* (1996) summarised in Fig. 8, suggest that the increasing stability of high-Al MgSiPvk may limit the lower mantle zone or mineral facies with garnet and/or TAPP to as little as ca. 2GPa or 60 km. Other experimental data (O'NEIL and JEANLOZ, 1994; KESSON *et al.*, 1995; MIYAJIMA *et al.*, 1996) suggest it is probably more than 100 km deep. HIROSE *et al.* (1999) show that the overlap in pressure of stability of MgSiPvk and garnet-majorite is only near 1GPa

for a MORB basic rock composition. They also point out that the phase relationships will vary from those of the simple $MgSiO_3$-$Mg_3Al_2Si_3O_{12}$ system as a function of other chemical components (such as Na) in the natural systems. The São Luiz inclusions emphasise that Fe^{3+}/Fe^t will be an important factor in these relationships.

Mineral facies for ultrabasic and basic rock compositions

In the preceding discussion we have shown that the São Luiz silicate (MgSiPvk, TAPP, SiO_2) and oxide (fPer) inclusions show regular features of association and composition which are compatible with phase equilibrium requirements and are in accord with much experimental data for the uppermost 100 km of the lower mantle. Consideration may now be given to the mineral assemblages expected in natural bulk rock compositions in the lower mantle. In Figs. 6 and 7 we plot estimated average mantle compositions based on chondritic and solar element abundances (ANDERSON, 1989); as well as pyrolite, primitive MORB and harzburgite bulk compositions used by IRIFUNE and RINGWOOD (1987) to model average mantle and subducted oceanic lithosphere mantle. The more usually adopted ultrabasic compositions all plot in the field of MgSiPvk-fPer ($\pm$TAPP) assemblages, but the solar mantle and the primitive MOR basalt compositions may be expected to carry SiO_2 in addition. Taking consideration of $Fe^{2+}/(Fe^{2+} + Fe^{3+})$ will move projected compositions in Figs. 6 and 7 to more magnesian positions, because the projections plot all Fe as FeO. Thus commonly expected ultrabasic (meta-peridotite or pyrolite) and basic (meta-basalt or meta-eclogite) compositions are likely to be constrained to MgSiPvk-bearing assemblages with fPer up to 0.30 $Fe^t(Fe^t + Mg)$ and MgSiPvk up to 0.11 $Fe^t(Fe^t + Mg)$.

In addition to the Mg-Fe-Al-Si-O phases discussed in detail (Figs. 6, 7 and 8), lower mantle ultrabasic and basic mantle compositions may be expected to carry a Ca-rich phase, which is CaSiPvk on the basis of the present inclusion data and experimental data (MAO *et al.*, 1989). In consideration of the phase relations, CaSiPvk is an extra phase stabilised by the extra component Ca, which is additional to Mg-Fe-Al-Si-O phases and components.

Based on both the experimental and the inclusion data one may distinguish two major mineral facies (ESKOLA, 1921) for the upper part of the lower mantle:

(i) A *low-Al MgSiPvk facies,* with limited Al solubility in MgSiPvk and a separate stable Al-silicate phase (garnet and /or TAPP).

(ii) A *high-Al MgSiPvk facies,* where all Al will be accommodated in MgSiPvk for normal ultrabasic and basic compositions (exceptional Al-rich compositions might contain corundum, Al_2O_3).

In the low-Al MgSiPvk facies, ultrabasic rocks are expected to carry the assemblage MgSiPvk + fPer + CaSiPvk ($\pm$Grt/TAPP, depending on the Al content and pressure-temperature conditions); whilst basic rock compositions will have assemblages of MgSiPvk + CaSiPvk + Grt/TAPP ($\pm$fPer or SiO_2, depending on bulk Si content). In the high-Al MgSiPvk facies, ultrabasic rocks will have MgSiPvk + fPer + $CaSiO_3$; whilst basic rocks have MgSiPvk + CaSiPvk ($\pm$ fPer or SiO_2).

Clearly, the distributions of the mineral assemblages noted above, coupled with the chemical compositions and elastic constants of the minerals, will determine the mechanical, dynamic and general geophysical properties of lower mantle rocks (*e.g.,* IRIFUNE and RINGWOOD, 1987, 1993; JEANLOZ and KNITTLE, 1989; JACOBS, 1992; WOOD and RUBIE, 1996; MCCAMMON, 1997; STIXRUDE *et al.*, 1992, 1998). The zone with a separate Al-silicate-phase at the top of the lower mantle is a crucial one from the viewpoint of the changing density relationships for ultrabasic and basic rock compositions and their relative propensity to sink (*e.g.,* RINGWOOD, 1988; IRIFUNE and RINGWOOD, 1993; HIROSE *et al.*, 1999). In the situation of layered mantle convection (*e.g.,* JACOBS, 1992) the garnet and/or TAPP stability zone will form part of the thermal boundary layer (*e.g.,* RICHTER and MCKENZIE, 1981; STACEY, 1992; BOEHLER, 1997) and the stability relations will be affected by a strong temperature gradient as well as pressure variation. Although the overall stability relations of garnet and TAPP are very important in this situation, the similarity in density characteristics of garnet and TAPP, means that the density changes of ultrabasic and basic compositions in this zone are not strongly modified by the occurrence of TAPP rather than garnet (HARRIS *et al.*, 1997).

DISCUSSION OF ORIGINS, P–T CONDITIONS AND MANTLE DYNAMICS

Original source materials, P–T conditions of equilibration and encapsulation in diamonds

In the preceding section, we have argued that where the phase relationships of the mineral associations containing fPer are well constrained, they indicate conditions of formation at shallow depths in the lower mantle. Effectively this is equivalent to noting the conditions of latest recrystallisation or metamorphism for the inclusion associations, and may potentially be distinguished from the na-

ture of the original source rock material (or proto-lith), which underwent the recrystallisation or metamorphism. Such a distinction is important, given that material within the mantle is clearly subject to displacement by convection, together with descent in subduction zones and ascent in plumes (*e.g.,* JACOBS, 1992).

A major proportion of the mineral inclusions released from São Luiz diamonds have shown shapes indicating imposed diamond morphology (WILDING, 1990; Hutchison, 1997). Such imposition of dominant host crystallographic faces upon inclusions is common with diamond hosts, and not only is it considered to show the crystalloblastic force of diamond faces, but to demonstrate that the *growth of both diamond and inclusion occurred simultaneously* (HARRIS and GURNEY, 1979). It is presumably partly for this reason that the diamonds tend to have inclusions which are each of a single mineral rather than a mineral aggregate. The formation of the diamond itself was most likely connected to ingress and reaction of a C-O-H fluid, probably with changing conditions of oxygen fugacity (DEINES, 1980). The evidence of simultaneous growth of diamond and inclusions, links encapsulation of the inclusions not only to a period of diamond growth, but to a period of recrystallisation or reconstitution of the material giving rise to the inclusions. Thus even though the source material for the inclusions may have undergone transport and modification in the mantle before the time of encapsulation in diamond, it must bear the imprint of the pressure-temperature and chemical conditions pertaining to the time of diamond growth. After encapsulation the included material was protected from further change in chemical composition, but its physical state may well have been affected by transport of the diamonds to a different pressure-temperature regime.

We therefore emphasise the point that the pressure-temperature conditions we have been able to define for the São Luiz inclusions refer to a period of mineral growth when the diamonds encapsulated the inclusions, and that this period of mineral growth (diamonds and inclusions) may be separate in time from that of the origin of some geochemical characteristics which refer to the initial source material for both the diamonds and the inclusions. Thus for any diamond-inclusion pair we might be able to distinguish two separate origins of material (one for diamond, one for inclusion), but will have only one set of pressure-temperature conditions for both minerals, which refers to the time of inclusion encapsulation.

Protoliths

We have shown that much of the inclusion material has chemical characteristics indicative of common mantle rocks of ultrabasic to basic composition, and that these are coupled with phase assemblages (mineral facies) expected for such material at uppermost lower mantle conditions. However, two specific features of geochemical composition, relating to $CaSiO_3$ and $(Mg,Fe)O$ inclusions, suggest the possibility of two very distinct origins (special protoliths) for parts of the São Luiz inclusion suite, and these are discussed in turn below.

A crustal origin for some CaSiPvk? The Eu anomaly found in the CaSiPvk inclusions is a very distinctive feature, and the best known circumstances of formation of such anomalies is associated with the crystallisation of feldspar within which divalent Eu is strongly partitioned. This implies an original source rock containing feldspar, and therefore most probably of crustal origin, which entered the mantle by subduction. One way of demonstrating that the Eu-anomaly derived from a previous protolith composition would be if the anomaly occurred in several of the lower mantle minerals forming the present assemblages. Unfortunately, the abundances of REE within the other minerals (MgSiPvk, fPer, TAPP) are too low to test this, since the low concentrations give large errors, which make the presence or absence of an Eu anomaly unclear for all minerals other than the CaSiPvk.

An alternative explanation to a crustal origin for the Eu anomaly, might relate to some intrinsic feature of $CaSiO_3$-perovskite crystal chemistry which affected Eu partitioning. However, it is notable that Eu anomalies are not normally associated with the ordinary $CaTiO_3$ perovskites of the upper mantle (MITCHELL, 1996). Thus, at present the most obvious explanation of the Eu anomalies is that the CaSiPvk inclusions indicate the presence of subducted crustal protolith material along the lower/upper mantle boundary; as might be expected if buoyancy relationships caused some accumulation at the top of the lower mantle of basic compositions, which were then spread laterally by convection (IRIFUNE and RINGWOOD, 1993; HIROSE *et al.*, 1999). The calculated São Luiz bulk trace element compositions (indicated by SLLM pyrolite in Fig. 4) are also compatible with this supposition.

A D″ origin for some (Mg,Fe)O inclusions? A most striking aspect of the São Luiz fPer is their wide range of $Fe^{2+}/(Fe^{2+} + Mg)$ compositions. Mantle compositions are expected to be Mg-rich, and as discussed above, mineral compositions would not

normally exceed 0.30 $Fe^{2+}/(Fe^{2+} + Mg)$. Considering only a mantle source region, a range of Mg-Fe compositions might be generated by crystal-melt fractionation processes, but the range of fPer compositions seen at São Luiz is extremely large and extends to 0.62 $Fe^{2+}/(Fe^{2+} + Mg)$. Furthermore, crystal-melt fractionation processes in the lower mantle are probably restricted given the high potential melting temperatures compared with likely geothermal gradients (ZERR and BOEHLER, 1994; BOEHLER, 1997; HIROSE et al., 1999); though this problem might be averted by imagining the differentiation processes as occurring in the upper mantle and being transported to the lower mantle by convection or subduction. Another difficulty facing a crystal-melt fractionation process is that the more Fe-rich fPer inclusions appear to have come from an environment less-rich in incompatible elements than the magnesian fPer (Fig. 5), which is the opposite of what might be expected for an evolved Fe-rich melt.

A potential way round the high Fe/Mg problem of some fPer would be to speculate that these compositions had come from the D'' zone of the mantle, adjacent to the Earth's core. KNITTLE and JEANLOZ (1991) and ZERR and BOEHLER (1994) have noted from experimental data the potential for interaction of (Mg,Fe)O with molten Fe at the core-mantle boundary. The Fe-rich material generated this way may then be transported to higher levels by uprising parts or plumes of mantle convection systems (e.g., LOPER and McCARTNEY, 1986; HOFMANN, 1997), and if convection is layered, with a boundary at the lower/upper mantle junction, then Fe-rich (Mg,Fe)O material from D'' may become entrained along that junction at a similar level to that from which silicates of the São Luiz lower mantle suite appear to derive.

Mantle dynamics

Matters concerning source rocks and pressure-temperature conditions of formation may now be viewed in the context of mantle dynamics. Under the pressure-temperature conditions obtaining in all the mantle except that of the lithosphere, a system of convective flow must clearly be expected (e.g., RICHTER and McKENZIE, 1981; JACOBS, 1992; CHRISTENSEN, 1995). What is less clear is whether the convective cells embrace the whole range of mantle depths below the lithosphere or whether convection is layered with separate circulatory systems in the upper and lower mantle. The question of the scale of mantle mixing is also linked to questions concerning subduction and plumes: do subducted slabs penetrate the lower mantle? and do the plumes giving rise to eruptive igneous rocks arise within the upper mantle

or may they come from the lower mantle? Figure 9 illustrates the two common alternative situations with 'whole' and 'layered' mantle convection.

RINGWOOD and IRIFUNE (1988) and IRIFUNE and RINGWOOD (1993) have extensively discussed the effects of the phase transformations occurring at the lower/upper mantle boundary, and noted that lower density basic material may tend to accumulate near the boundary whilst ultrabasic material sinks, thus causing differentiation between subducted materials at this depth. Geodynamic arguments are strongly dependent on the magnitude of the changes of the physical properties at the lower/upper mantle boundary (CHRISTENSEN, 1995; FORTE and WOODWARD, 1997). Recent seismic evidence has favoured the continuation of subducted material into the lower mantle (VAN DER HILST et al., 1997; GRAND et al., 1997), and it may be that such material accumulating in D'' causes distinctive seismic characteristics for that zone (LOPER and LAY, 1995; KENDALL and SILVER, 1996). HAGGERTY (1994) argues for the generation of some plumes or superkimberlites at the core mantle boundary and the entrainment of D'' material. On the other hand geochemical evidence concerning maintenance of a primary compositional reservoir for the isotopes of inert gases and the U-Pb-Th system has supported the concept of dominantly separate upper and lower mantle convective systems (O'NIONS, 1987; McKENZIE and O'NIONS, 1995; HOFMANN, 1997). For some aspects of geochemistry the question of whether subducted material reaches the lower mantle is crucial, in that the isotopic signature of some basaltic eruptive rocks has been linked to distinctive chemical features in subducted material (HOFMANN and WHITE, 1982; HOFMANN, 1997). STEIN and HOFMANN (1994) have suggested that there may be periodic changes in the scale of mantle convection systems.

On the basis of the evidence of the special protoliths, the São Luiz inclusions suggest a mixture of source material, derived not only from standard mantle compositions, but also from protolith compositions originating in the top (crust) and bottom (D'') bounding systems of the mantle. In the case of whole mantle convection, the obvious location for mixing subducted crustal material and D'' material is in D'' (Fig. 9); whilst in the case of layered mantle convection it is along the lower/upper mantle boundary. Thus the protolith evidence alone does not provide a means of discriminating between the two convection systems, since plumes originating at either the core mantle boundary or the lower/upper mantle boundary could carry both types of material.

The pressure-temperature conditions of growth and encapsulation in diamond of the included min-
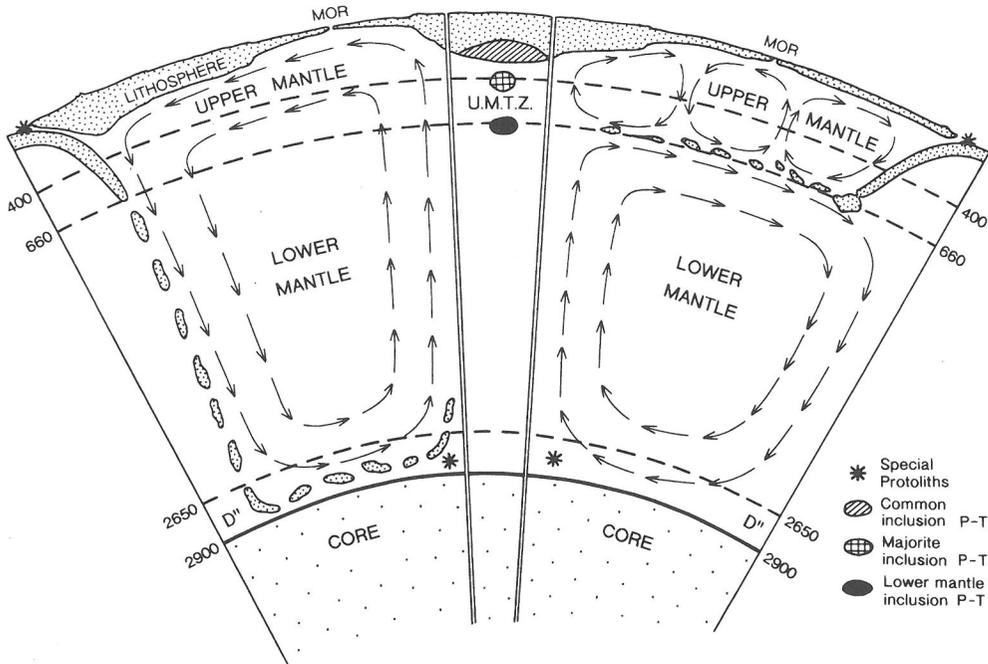
FIG. 9. Diagrammatic illustration (approximately to scale) of: *left panel* - whole mantle convection with subducted material penetrating the lower mantle and incorporated in D″; *right panel*—layered mantle convection with subducted material spread out along the lower/upper mantle boundary. In both left and right panels the original positions of formation of special protoliths (material with Eu anomalies in the crust, and Fe-rich Mg-Fe oxides in D″—see text) are indicated. The small *centre panel* shows: the particular P–T conditions of formation indicated by São Luiz lower mantle inclusions, the P–T conditions of formation indicated by Sao Luiz majorite inclusions, the common P–T conditions of formation of most diamond inclusions worldwide (though not abundant at São Luiz). U.M.T.Z. is upper mantle transition zone.

erals provide stronger constraints. The associations of the MgSiPvk, fPer, TAPP, and SiO₂ inclusions demonstrate pressure-temperature conditions in the uppermost lower mantle, and it is possible that all the mineral inclusions described herein could have formed and been trapped in diamonds in the uppermost 100 km of the lower mantle. In the case of layered mantle convection this zone would lie in the thermal boundary layer (RICHTER and MCKENZIE, 1981; BOEHLER, 1997) at the contact of the upper and lower mantle cells (Fig. 9). If all the inclusions were encapsulated in diamond adjacent to the lower/upper mantle boundary, then it follows that mixing of subducted and D″ material must have occurred along this zone and that layered mantle convection is indicated. Evidence from convection modelling shows that horizontal transport along the boundary layers is relatively rapid and that entrained material tends to remain within the boundary layers rather than moving to the interior of the convection cells (MCKENZIE and O'NIONS, 1995). Clear evidence that material of diverse origins was mixed together along the lower/

upper mantle boundary at uppermost lower mantle pressure-temperature conditions, is provided by diamond BZ205, where a magnesian fPer and TAPP (inclusions BZ205B and BZ205A) are associated with a decidedly Fe-rich fPer (inclusion BZ206C).

The loopholes in the above argument are that we cannot prove that the CaSiPvk carrying Eu anomalies and the Fe-rich fPer were trapped in diamond near the lower/upper mantle boundary. Taking these inclusions individually, the pressure-temperature equilibria allow formation over the range of lower mantle conditions and even in the lowermost upper mantle. One could further argue that there may be other (albeit uncertain) ways of forming Eu anomalies and extreme Fe enrichment, besides the crustal and D″ origins noted. That inclusions within diamonds from the São Luiz alluvial suite have been sampled from more than one mantle depth is demonstrated by the occurrence of an inclusion suite of majoritic garnets (WILDING *et al.*, 1991; HARTE, 1992) from the upper mantle transition zone (U.M.T.Z. in Fig. 9). But this may be countered by noting that the bulk composi-

tions of the lower mantle suite diamonds have narrowly defined $\delta^{13}C$ and nitrogen characteristics, suggesting a closely linked grouping which is distinct from that of the diamonds with majorite characteristics (WILDING, 1990; HUTCHISON *et al.*, 1998).

On balance, the evidence of pressure-temperature conditions of formation in the uppermost lower mantle, coupled with the homogeneity of the diamond suite carrying lower mantle inclusions, argues for encapsulation of all these inclusions in diamond adjacent to the lower/upper mantle boundary; and in conjunction with the evidence of both subducted crustal and D″ protolith material in the suite, this then supports the occurrence of layered mantle convection.

CONCLUSIONS

A suite of alluvial diamonds from São Luiz contain inclusions of (Mg,Fe)O oxide together with silicates phases having the compositions: (a) $(Mg,Fe)SiO_3$, (b) $CaSiO_3$, (c) $(Mg,Fe)_3Al_2Si_3O_{12}$, (d) SiO_2.

Associations of these phases in the same diamonds indicate that they represent largely expected lower mantle mineral assemblages of periclase-wüstite (fPer) with (Mg,Fe)Si-perovskite (MgSiPvk) , CaSi-perovskite (CaSiPvk), TAPP (a tetragonal aluminous phase with garnet-like composition) and stishovite.

The principal departure from experimentally predicted relations is the occurrence of the TAPP phase rather than a majoritic garnet composition.

Mg-Fe partitioning between phases shows consistent relationships so long as Fe^{3+}/Fe^t is taken into account, with high Fe^{3+}/Fe^t in the silicates and low Fe^{3+}/Fe^t in fPer.

Minor element and trace element partitioning shows consistent relationships, in accord with experimental evidence. The REE are strongly partitioned into CaSiPvk.

Carbon isotope measurements on the host diamonds show normal mantle $\delta^{13}C$ compositions, whilst N contents are characteristically low or absent and suggest a distinct source. $\delta^{18}O$ measurements on one CaSiPvk also show expected mantle compositions.

A consistent set of phase relationships in the system $MgO-FeO-Al_2O_3-SiO_2$ may be derived from the inclusions, by assuming that inclusions within one diamond are generally in equilibrium with one another. CaSiPvk may be considered as an additional phase, stabilised by the addition of CaO to the above system.

Associations of MgSiPvk and TAPP with fPer are restricted to magnesian compositions with co-existing fPer containing up to 30% $Fe^{2+}/(Fe^{2+} + Mg)$.

The relationships seen in $MgO-FeO-Al_2O_3-SiO_2$ show good agreement with experimental data on phase assemblages in the uppermost lower mantle, but with the TAPP phase occurring in place of majorite garnet.

The phase data indicate two mineral facies: (i) with MgSiPvk co-existing with TAPP as aluminous phase; (ii) with an aluminous MgSiPvk and no separate aluminous silicate (in both facies it is possible that Al_2O_3 might occur in exceptionally aluminous compositions).

Experimental data show that these associations (facies) are to be expected over a small range of increasing pressure in the uppermost part of the lower mantle, and it is most probable that the inclusions became encapsulated and preserved within diamonds in this region.

The inclusions therefore provide important natural evidence on phases and phase compositions that may be used in modelling geochemical and geophysical characteristics for the uppermost lower mantle.

Two distinct protoliths, apart from expected mantle ultrabasic-basic compositions, are indicated for the inclusion suite: (i) crustal protoliths marked by positive Eu anomalies; (ii) D″ protoliths indicated by extreme Fe-rich compositions in some fPer.

Assuming the aforesaid encapsulation within diamond in the uppermost lower mantle, the inclusions suggest mixing of diverse crustal, mantle and D″ material along the upper/lower mantle boundary, and therefore support the occurrence of layered mantle convection.

REFERENCES

AHMED-ZAID I. and MADON M. (1995) Electron microscopy of high-pressure phases synthesised from natural garnets in a diamond anvil cell: implications for the mineralogy of the lower mantle. *Earth Planet Sci. Lett.* **129,** 233–247.
ANDERSON D. L. (1989) *Theory of the Earth.* Blackwell, Boston.
BOEHLER R. (1997) The temperature in the Earth's core. In *Earth's Deep Interior* (ed. D. J. CROSSLEY), pp. 51–63, Gordon and Breach Science Publishers, Amsterdam.
CHAZOT G., LOWRY D., MENZIES M., and MATTEY D. (1997) Oxygen isotopic composition of hydrous and anhydrous

mantle peridotites. *Geochim. Cosmochim. Acta* **61**, 161–169.

CHRISTENSEN U. R. (1995) Effect of phase transitions on mantle convection. *Annual Rev. Earth Planet. Sci.* **23**, 65–87.

DEINES P. (1980) The carbon isotopic composition of diamonds: relationship to diamond shape, color, occurrence and vapor composition. *Geochim. Cosmochim. Acta* **44**, 943–961.

DUFFY T. and ANDERSON D. (1989) Seismic velocities in mantle minerals and the mineralogy of the upper mantle. *J. Geophys. Res.* **94**, 1895–1912.

ESKOLA P. (1921) On the eclogites of Norway. *Oslo Vidensk. Skr., I, Mat.-Naturw. Kl.* **8**, 1–118.

FEI Y., MAO H. K., and MYSEN B. O. (1991) Experimental determination of element partitioning and calculation of phase relations in the MgO-FeO-SiO₂ system at high pressure and high temperature. *J. Geophys. Res.* **96**, 2157–2169.

FEI Y., WANG Y., and FINGER L. W. (1996) Maximum solubility of FeO in (Mg, Fe)SiO₃-perovskite as a function for FeO content in the lower mantle. *J. Geophys. Res.* **101**, 11525–11530.

FORTE A. M. and WOODWARD R. L. (1997) Siesmic-geodynamic constraints on vertical flow between the upper and loer mantle: the dynamics of the 670 km seismic discontinuity. In *Earth's Deep Interior* (ed. D. J. CROSSLEY), pp. 337–404, Gordon and Breach Science Publishers, Amsterdam.

GRAND S. P., VAN DER HILST R. D., and WIDIYANTORO S. (1997) Global seismic tomography: A snapshot of convection in the Earth. *Geol. Soc. Am. Today* **7**, 1–7.

GURNEY J. J. (1989) Diamonds. In *Kimberlites and Related Rocks* (eds. J. ROSS *et al.*), pp. 935–965, Blackwell, Victoria.

GUYOT F., MADON M., PEYRONNEAU J., and POIRIER J. P. (1988) X-ray microanalysis of high-pressure high-temperature phases synthesised from natural olivine in a diamond-anvil cell. *Earth Planet. Sci. Lett.* **90**, 52–64.

HAGGERTY S. E. (1994) Superkimberlites: a geodynamic diamond window to the Earth's core. *Earth Planet. Sci. Lett.* **122**, 57–69.

HARRIS J. W. (1987) Recent physical, chemical and isotopic research of diamond. In *Mantle Xenoliths* (ed. P. H. NIXON). John Wiley and Sons, Chichester.

HARRIS J. W. and GURNEY J. (1979) Inclusions in diamonds. In *Properties of Diamond* (ed. J. E. FIELD), pp. 555–591, Academic, London.

HARRIS J. W., HUTCHISON M. T., HURSTHOUSE M., LIGHT M., and HARTE B. (1997) A new tetragonal silicate mineral occuring as inclusions in lower-mantle diamonds. *Nature* **387**, 486–488.

HARTE B. (1982) Mantle peridotites and processes - the Kimberlite sample. In *Continental Basalts and Mantle Xenoliths* (eds. C. J. HAWKESWORTH and M. J. NORRY), pp. 46–91, Shiva, Nantwich.

HARTE B. (1992) Trace element characteristics of deep-seated eclogitic parageneses - an ion microprobe study of inclusions in diamonds. *Abstrs. V. M. Goldschmidt Conf.*, A–48.

HARTE B. and HARRIS J. W. (1994) Lower mantle mineral associations preserved in diamonds. *Mineral. Mag.* **A58**, 384–385.

HARTE B. and KIRKLEY M. B. (1997) Parttioning of trace elements between clinopyroxene and garnet: data from mantle eclogites. *Chem. Geol.* **136**, 1–24.

HARTE B., HUTCHISON M. T., AND HARRIS J. W. (1994)

Trace element characteristics of the lower mantle: an ion probe study of inclusions in diamonds from São Luiz, Brazil. *Mineral. Mag.* **A58**, 386–387.

HARTE B., HUTCHISON M. T., LEE M., and HARRIS J. W. (1998) Inclusions of (Mg,Fe)O in mantle diamonds. *Extd Abstrs. 7th Int. Kimb. Conf.*, 308–310.

HIROSE K., FEI Y., MA Y., and MAO H-K. (1999) Fate of subducted basaltic crust in the lower mantle. *Nature* **397**, 53–56.

HOFMANN A. W. (1997) Mantle geochemistry: the message from oceanic volcanism. *Nature* **385**, 219–229.

HOFMANN A. W. and WHITE W. M. (1982) Mantle plumes from ancient oceanic crust. *Earth Planet. Sci. Lett.* **57**, 421–436.

HUTCHISON M. T. (1997) *Constitution of the Deep Transition Zone and Lower Mantle Shown by Diamonds and Their Inclusions.* Ph. D. thesis, University of Edinburgh.

HUTCHISON M. T., CARTIGNY P., and HARRIS J. W. (1998) Carbon and nitrogen compositions and cathodoluminescence characteristics of transition zone and lower mantle diamonds from São Luiz, Brazil. *Extd Abstrs. 7th Int. Kimb. Conf.*, 336–338.

IRIFUNE T. and RINGWOOD A. E. (1987) Phase transformations in a harzburgite composition to 26 GPa: implications for dynamical behaviour of the subducting slab. *Earth Planet. Sci. Lett.* **86**, 365–376.

IRIFUNE T. and RINGWOOD A. E. (1993) Phase transformations in subducted oceanic crust and buoyancy relationships at depths of 600–800 km in the mantle. *Earth Planet. Sci. Lett.* **117**, 103–110.

IRIFUNE T. (1994) Absence of an aluminous phase in the upper part of the earth's lower mantle. *Nature* **270**, 131–133.

IRIFUNE T., KOIZUMI T., and ANDO J-I. (1996) An experimental study of the garnet-perovskite transformation in the system MgSiO₃-Mg₃Al₂SiO₁₂. *Phys. Earth Planet. Inter.* **96**, 147–157.

IRIFUNE T., SEKINE T., RINGWOOD A. E., and HIBBERSON W. O. (1986) The eclogite-garnetite transformation at high pressure and some geophysical implications. *Earth Planet. Sci. Lett.* **77**, 245–256.

ITO E. and TAKAHASHI E. (1987) Ultrahigh-pressure phase transformations and the constitution of the deep mantle. In *High-Pressure Research in Mineral Physics* (eds. M. H. MANGHNANI and Y. SYONO), pp. 221–229, Terrapub, Tokyo.

ITO E. and TAKAHASHI E. (1989) Postspinel transformations in the system Mg₂SiO₄-Fe₂SiO₄ and some geophysical implications. *J. Geophys. Res.* **94**, 10637–10646.

JACOBS J. A. (1992) *Deep Interior of the Earth.* Chapman & Hall, London.

JEANLOZ R. and KNITTLE E. (1989) Density and composition of the lower mantle. *Philos. Trans. R. Soc. London* **A328**, 328, 377.

KATO T., RINGWOOD A. E., and IRIFUNE T. (1988) Experimental determination of element partitioning between silicate pervoskites, garnets and liquids: Constraints on early differentiation of the mantle. *Earth Plan. Sci. Lett.* **89**, 123–145.

KATO T., OHTANI E., ITO Y., and ONUMA K. (1996) element partitioning between silicate perovskites and calcic ultrabasic melt. *Phys. Earth Planet. Inter.* **96**, 201–207.

KENDALL J. M. AND SILVER P. G. (1996) Constraints from seismic anisotropy on the nature of the lowermost mantle. *Nature* **381**, 409–412.

KESSON S. E. and FITZGERALD J. D. (1991) Partitioning of MgO, FeO, NiO, MnO and Cr₂O₃ between magnesian sil-

icate pervoskite and magnesiowüstite: implications for the origin of inclusions in diamond and the composition of the lower mantle. *Earth Planet. Sci. Lett.* **111,** 229–240.

KESSON S. E., FITZGERALD J. D., SHELLEY J. M. G., and WITHERS R. L. (1995) Phase relations, structure and crystal chemistry of some aluminous silicate perovskites. *Earth Planet. Sci. Lett.* **134,** 187–201.

KNITTLE E. and JEANLOZ R. (1991) Earth's core-mantle boundary: results of experiments at high pressures and temperatures. *Science* **251,** 1438–1440.

LIU L. G. (1975) Post-oxide phases of olivine and pyroxene and mineralogy of the mantle. *Nature* **258,** 510–512.

LOPER D. E. and LAY T. (1995) The core mantle boundary region. *J. Geophys. Res.* **100,** 6397–6420.

LOPER D. E. and MCCARTNEY K. (1986) Mantle plumes and the periodicity of magnetic field reversals. *Geophys. Res. Lett.* **13,** 1525–1528.

LLOYD G. E. (1987) Atomic number and crystallographic contrast images with SEM: A review of backscattered electron techniques. *Mineral. Mag.* **51,** 3–19.

MAO H. K., CHEN L. C., HEMLEY R. J., JEPHCOAT A. P., WU Y., and BASSETT W. A. (1989) Stability and equation of state of CaSiO$_3$-pervoskite to 134 GPa. *J. Geophys. Res.* **94,** 17889–17894.

MATTEY D., LOWRY D., and MACPHERSON C. (1994) Oxygen isotope composition of mantle peridotite. *Earth Planet. Sci. Lett.* **128,** 231–241.

MCCAMMON C. A. (1997) Perovskite as a possible sink for ferric iron in the lower mantle. *Nature* **387,** 694–696.

MCCAMMON C. A., HARRIS J. W., HARTE B., and HUTCHISON M. T. (1995) Ferric iron content of (Fe,Mg)O from lower mantle inclusions. (abstr.) *Terra Nostra* **3,** 91.

MCCAMMON C. A., HUTCHISON M. T., and HARRIS J. W. (1997) Ferric iron content of mineral inclusions in diamonds from São Luiz: A view into the lower mantle. *Science* **278,** 434–436.

MCCAMMON C. A., PEYRONNEAU J., and POIRIER J.-P. (1998) Low ferric iron content of (Mg,Fe)O at high pressures and temperatures. *Geophys. Res. Lett.* **25,** 1589–1592.

MCDADE P. and HARRIS J. W. (in press) Syngenetic inclusion bearing diamonds from Letseng-La-Terai, Lesotho. *Proc. Seventh Int. Kimb. Conf.*

MCDONOUGH W. F. and SUN S.-S. (1995) The composition of the Earth. *Chemical Geology* **120,** 223–253.

MCKENZIE D. and O'NIONS R. K. (1995) The source regions of ocean island basalts. *J. Petrol.* **36,** 133–160.

MEYER H. O. A. (1987) Inclusions in diamond. In *Mantle Xenoliths* (ed. P. H. NIXON), pp. 501–522, John Wiley & Sons, Chichester.

MITCHELL R. H. (1996) Pervoskites: a revised classification scheme for an important rare earth element host in alkaline rocks. In *Rare Earth Minerals* (eds. A. P. JONES, F. WALL, and C. T. WILLIAMS), pp. 41–76, Chapman & Hall, London.

MIYAJIMA N., FUJINO K., YAGI T., and KONDO T. (1996) Analytical electron mciroscopy of garnet-perovskite transformation in a laser-heated diamond anvil cell. In *Proc. 3rd NIRM Int. Symp. on Advanced Materials* (eds. AKAISHI *et al.*), pp. 341–344. National Institute for Research in Inorganic Materials, Tsukuba.

MOORE R. O., OTTER M. L., RICKARD R. S., HARRIS J. W., and GURNEY J. J. (1986) The occurrence of moissanite and ferro-periclase as inclusions in diamond. *Geol. Soc. Aust. Abstr.* **16,** 409–411.

O'NEILL B. and JEANLOZ R. (1994) MgSiO$_3$-FeSiO$_3$-Al$_2$O$_3$ in the Earth's lower mantle: Perovskite and garnet at 1200 km depth. *J. Geophys. Res.* **99,** 19901–19915.

O'NEILL H. ST. C., MCCAMMON C. A., CANIL D., RUBIE D. C., ROSS C. R. II and SEIFERT F. (1993) Mössbauer spectroscopy of mantle transition zone phases and determination of minimum Fe^{3+} content. *Amer. Mineral.* **78,** 456–460.

O'NIONS R. K. (1987) Relationships between chemical and convective layering in the Earth. *J. Geol. Soc.* **144,** 259–274.

OTTER M. L. and GURNEY J. J. (1989) Mineral Inclusions in diamond from the Sloan diatremes, Colorado-Wyoming State Line kimberlite district, North America. In *Kimberlites and Related Rocks* (eds. J. ROSS *et al.*), Vol. **2,** pp. 1042–1053, Blackwell, Victoria.

POIRIER J.-P. (1991) *Introduction to Physics of the Earth's Interior.* Cambridge University Press.

RICHTER F. and MCKENZIE D. (1981) On some consequences and possible causes of layered mantle convection. *J. Geophys. Res.* **86,** 6133–6142.

RICHMOND N. C. and BRODHOLT J. P. (1998) Calculated role of aluminum in the incorporation of ferric iron into magnesium silicate perovskite. *Amer. Mineral.* **83,** 947–951.

RINGWOOD A. E. (1982) Phase transformations and differentiation in subducted lithosphere: Implications for mantle dynamics, basalt petrogenesis and crustal evolution. *J. Geol.* **90,** 611–643.

RINGWOOD A. E. and IRIFUNE T. (1988) Nature of the 650-km seismic discontinuity: implications for mantle dynamics and differentiation. *Nature* **331,** 131–136.

SCOTT-SMITH B. H., DANCHIN R. V., HARRIS J. W., and STRACKE K. J. (1984) Kimberlites near Orroroo, South Australia. In *Kimberlites I: Kimberlites and Related Rocks* (ed. J. KORNPROBST), pp. 121–242, Elsevier, Amsterdam.

SHEARER P. M. and MASTERS T. G. (1992) Global mapping of topography on the 660 km discontinuity. *Nature* **355,** 791–795.

STACHEL T., HARRIS J. W., and BREY G. P. (1998) Rare and unusual mineral inclusions in diamonds from Mwadui, Tanzania. *Contrib. Mineral. Petrol.* **132,** 34–47.

STACEY F. D. (1992) *Physics of the Earth.* Brookfield Press, Kenmore, Queensland, Australia

STEIN M. and HOFMANN A. W. (1994) Mantle plumes and episodic crustal growth. *Nature* **372,** 63–68.

STIXRUDE L., HEMLEY R. J., FEI Y., and MAO H. K. (1992) Thermoelasticity of silicate perovskite and magnesiowüstite and stratification of the Earth's mantle. *Science* **257,** 1099–1101.

STIXRUDE L. (1998) Elastic constants and anisotropy of MgSiO$_3$ pervoskite, periclase, and SiO$_2$ at high pressure. In *Core-Mantle Boundary* (eds. GURNIS *et al.*), AGU, Washington, DC.

SUN S.-S. and MCDONOUGH W. F. (1989) Chemical and isotopic systematics of oceanic basalts: implications for mantle composition and processes. In *Magmatism in Ocean Basins* (eds. A. D. SAUNDERS and M. J. NORRY), pp. 313–345, Geological Society, London.

TAKAHASHI E. and ITO E. (1987) Mineralogy of mantle peridotite along a model geotherm up to 700 km depth. In *High Pressure Research in Mineral Physics* (eds. M. H. MANGHNANI and Y. SYONO), pp. 427–438, American Geophysical Union, Washington, DC.

THOMPSON J. B. JR. (1957) The graphical analysis of mineral assemblages in pelitic schists. *Am. Mineral.* **42,** 842–858.

VALLEY J. W., GRAHAM C. M., HARTE B., EILER J. M., and KINNY P. D. (1998) Ion microprobe analysis of oxygen, carbon, and hydrogen isotope ratios. In *Applications of Microanalytical Techniques to Understanding Mineral-*

izing Processes (eds. M. A. McKIBBEN *et al.*), *Reviews in Economic Geology* **7**, 73–98.

VAN DER HILST R. D., WIDIYANTORO S., and ENGDAHL E. R. (1997) Evidence for deep mantle circulation from global tomography. *Nature* **386**, 578–584.

WANG Y., WEIDNER D. J., LIEBERMANN R. C., and ZHAO Y. (1994) *P-V-T* equation of state of $(Mg,Fe)SiO_3$ perovskite: constraints on composition of the lower mantle. *Phys. Earth Planet. Inter.* **83**, 13–40.

WATT G., HARRIS J. W., HARTE B., and BOYD S. (1994) A high-chromium corundum (ruby) inclusion in diamond from the São Luiz alluvial mine, Brazil. *Mineralog. Mag.* **58**, 490–492.

WILDING M. C. (1990) *A Study of Diamonds with Syngenetic Inclusions.* Ph. D. thesis, University of Edinburgh.

WILDING M. C., HARTE B., and HARRIS J. W. (1991) Evidence for a deep origin for São Luiz diamonds. *Extd. Abstrs. 5th Int. Kimb. Conf.,* 456–458.

WOOD B. J. and RUBIE D. C. (1996) The effect of alumina on phase transformations at the 660-kilometer discontinuity from Fe-Mg partitoning experiments. *Science* **273**, 1522–1524.

YAGI T., BELL P. M., and MAO H. K. (1979) Phase relations in the system $MgO-FeO-SiO_2$ between 150 and 700 kbar at 1000 °C, *Year Book, Carnegie Inst. Washington* **78**, 614–618.

ZERR A. and BOEHLER R. (1994) Constraints on the melting temperature of the lower mantle from high pressure experiments on MgO and magnesiowustite. *Nature* **371**, 506–508.